CANADIAN THESES ON MICROFICHE

THÈSES CANADIENNES SUR MICROFICHE

National Library of Canada
Collections Development Branch

Canadian Theses on
Microfiche Service

Ottawa, Canada
K1A 0N4

Bibliothèque nationale du Canada
Direction du développement des collections

Service des thèses canadiennes
sur microfiche

NOTICE

The quality of this microfiche is heavily dependent upon the quality of the original thesis submitted for microfilming. Every effort has been made to ensure the highest quality of reproduction possible.

If pages are missing, contact the university which granted the degree.

Some pages may have indistinct print especially if the original pages were typed with a poor typewriter ribbon or if the university sent us an inferior photocopy.

Previously copyrighted materials (journal articles, published tests, etc.) are not filmed.

Reproduction in full or in part of this film is governed by the Canadian Copyright Act, R.S.C. 1970, c. C-30. Please read the authorization forms which accompany this thesis.

AVIS

La qualité de cette microfiche dépend grandement de la qualité de la thèse soumise au microfilmage. Nous avons tout fait pour assurer une qualité supérieure de reproduction.

S'il manque des pages, veuillez communiquer avec l'université qui a conféré le grade.

La qualité d'impression de certaines pages peut laisser à désirer, surtout si les pages originales ont été dactylographiées à l'aide d'un ruban usé ou si l'université nous a fait parvenir une photocopie de qualité inférieure.

Les documents qui font déjà l'objet d'un droit d'auteur (articles de revue, examens publiés, etc.) ne sont pas microfilmés.

La reproduction, même partielle, de ce microfilm est soumise à la Loi canadienne sur le droit d'auteur, SRC 1970, c. C-30. Veuillez prendre connaissance des formules d'autorisation qui accompagnent cette thèse.

THIS DISSERTATION
HAS BEEN MICROFILMED
EXACTLY AS RECEIVED

LA THÈSE A ÉTÉ
MICROFILMÉE TELLE QUE
NOUS L'AVONS REÇUE

NL 339 (r. 85/09)

Canada

0-315-19569-X

National Library of Canada
Canadian Theses Division
Ottawa, Canada
K1A 0N4

Bibliothèque nationale du Canada
Division des thèses canadiennes

227

67477

PERMISSION TO MICROFILM — AUTORISATION DE MICROFILMER

• Please print or type — Écrire en lettres moulées ou dactylographier

Full Name of Author — Nom complet de l'auteur

DOO-PYO HONG

Date of Birth — Date de naissance

MARCH 31, 1948

Country of Birth — Lieu de naissance

KOREA

Permanent Address — Résidence fixe

297 GREENOCH CRESCENT
EDMONTON, AB. T6L 1W6

Title of Thesis — Titre de la thèse

VIBRATION ANALYSIS OF PERIODIC STRUCTURES

University — Université

UNIV. OF ALBERTA

Degree for which thesis was presented — Grade pour lequel cette thèse fut présentée

Ph.D.

Year this degree conferred — Année d'obtention de ce grade

1983

Name of Supervisor — Nom du directeur de thèse

DR. FAULKNER, M. G.

Permission is hereby granted to the NATIONAL LIBRARY OF CANADA to microfilm this thesis and to lend or sell copies of the film.

The author reserves other publication rights, and neither the thesis nor extensive extracts from it may be printed or otherwise reproduced without the author's written permission.

L'autorisation est, par la présente, accordée à la BIBLIOTHÈQUE NATIONALE DU CANADA de microfilmer cette thèse et de prêter ou de vendre des exemplaires du film.

L'auteur se réserve les autres droits de publication; ni la thèse ni de longs extraits de celle-ci ne doivent être imprimés ou autrement reproduits sans l'autorisation écrite de l'auteur.

Date

Oct. 14, 1983

Signature

Doo P. Hong

NL-91 (4/77)

THE UNIVERSITY OF ALBERTA

VIBRATION ANALYSIS OF PERIODIC STRUCTURES

by

DOO P. HONG

(C)

A THESIS

SUBMITTED TO THE FACULTY OF GRADUATE STUDIES AND RESEARCH

IN PARTIAL FULFILMENT OF THE REQUIREMENTS FOR THE DEGREE

OF Doctor of Philosophy

Mechanical Engineering

EDMONTON, ALBERTA

Fall 1983

THE UNIVERSITY OF ALBERTA

RELEASE FORM

NAME OF AUTHOR DOO P. HONG

TITLE OF THESIS VIBRATION ANALYSIS OF PERIODIC STRUCTURES

DEGREE FOR WHICH THESIS WAS PRESENTED Doctor of Philosophy

YEAR THIS DEGREE GRANTED Fall 1983

Permission is hereby granted to THE UNIVERSITY OF ALBERTA LIBRARY to reproduce single copies of this thesis and to lend or sell such copies for private, scholarly or scientific research purposes only.

The author reserves other publication rights, and neither the thesis nor extensive extracts from it may be printed or otherwise reproduced without the author's written permission.

(SIGNED) Doo P. Hong

PERMANENT ADDRESS:

297 Greenoch Crescent
Edmonton, Alberta
T6L 1W6

DATED Oct. 12 1983

THE UNIVERSITY OF ALBERTA

FACULTY OF GRADUATE STUDIES AND RESEARCH

The undersigned certify that they have read, and recommend to the Faculty of Graduate Studies and Research, for acceptance, a thesis entitled VIBRATION ANALYSIS OF PERIODIC STRUCTURES submitted by DOO P. HONG in partial fulfilment of the requirements for the degree of Doctor of Philosophy.

Gary Faulkner
Supervisor

External Examiner

Date October 12, 1983

ABSTRACT

The transfer matrix method employed for vibration analysis of periodic structure in the present study is somewhat similar in principle to the classical transfer matrix method which has long been used for a continuous beam on multiple supports (either spring or knife-edge supports). However, improvements are made on the method by combining the classical transfer matrix method with the concept of the propagation constant and the Finite Element formulation of an impedance matrix. The Finite Element formulation enables one to do the vibration analysis no matter how complex the structure may be; while the use of transfer matrices reduces the computational effort virtually to that of a single periodic unit.

The propagation constant which is obtained in the form of a logarithmic eigenvalue of the transfer matrix helps in the understanding of the vibration by indicating which flexural waves attenuate and which propagate along the periodic structure. Consequently, vibration problems of periodic structures which could be very difficult to analyze by other methods can be more easily and efficiently analyzed by this improved transfer matrix method.

The numerical examples taken in the present study are mostly for uniform Timoshenko beams with different intermediate supports and extreme boundary conditions. The natural frequencies or the steady-state forced harmonic response of such beams are obtained and the effect of rotary

inertia and shear deformation on the flexural motions of a multi-span beam is investigated. The application of the present method is by no means restricted to the uniform beam vibration problems. However, the numerical examples and their results may sufficiently demonstrate the versatility and superiority of the present method over other available methods for analysis of vibration of periodic structures.

Acknowledgment

Thanks to the Lord who gives all the courage and strength needed to complete the study.

For the long endurance, the Author thanks to his wife and family.

Thanks are also due to Dr. Faulkner for his kind advices and supervision.

Many helps and suggestions from the fellow graduate students are also acknowledged.

Table of Contents

Chapter Page

I. INTRODUCTION AND LITERATURE SURVEY 1

A. Periodic Structure 1

B. Transfer Matrix 2

C. Propagation Constant 4

D. Finite Element Method 6

E. Timoshenko Beam 8

II. TRANSFER MATRIX AND PROPAGATION CONSTANT 10

A. Introduction 10

B. Transfer Matrix from Impedance Matrix 12

C. Properties of Transfer Matrix 15

Inversion 15

Eigenvalues and Eigenvectors 17

Multiplication of transfer matrices 18

D. Propagation Constants and Transfer Matrix 20

E. Discussion 21

III. HARMONIC MOTIONS OF PERIODIC STRUCTURES 27

A. Introduction 27

B. Natural Frequencies 30

C. Steady-state Harmonic Response 32

D. Mono-coupled System 35

E. Discussion 48

IV. NUMERICAL EXAMPLE - UNIFORM TIMOSHENKO BEAM 55

A. Introduction 55

B. Analytical Formulation of Transfer Matrix 57

Timoshenko beam differential equation 57

Impedance matrix 62
Transfer matrix and its inverse 63
C. Special Cases 65
D. Natural Frequencies 67
Timoshenko beams on knife-edge supports 67
Timoshenko beams on elastic springs 73
E. Steady-state Harmonic Responses 76
Timoshenko beams on knife-edge supports 76
Timoshenko beams on elastic springs 83
F. Numerical Results by Finite Element Method 88
G. Discussion 94
V. CONCLUDING REMARKS 104
BIBLIOGRAPHY 107
VI. APPENDIX 109
A. Impedance matrices for spring-mass systems 109
B. Derivation of transfer matrix by direct method 111
C. Derivation of the reduced transfer matrix 112

List of Figures

Figure page

1.1. Examples of periodic structures;
(a) A simple periodic structure.
(b) A compound periodic structure 3

2.1. Block diagram of a periodic structure showing the generalized displacements and forces 12

3.1. Uniform beams with end elements different from the periodic element;
(a) End transfer matrices are required.
(b) End transfer matrices are not required 29

3.2. Harmonically excited infinite systems;
(a) Semi-infinite system.
(b) Infinite-infinite system 34

3.3. Examples of mono-coupled systems showing two possible element divisions;
(a) A spring-mass oscillating system.
(b) A uniform beam on knife-edge supports 36

3.4. Propagation constant for a spring-mass system 39

3.5. Free vibrations of a four span spring-mass system of symmetric elements;
(a) Free-free boundary.
(b) Free-fixed boundary.
(c) Fixed-fixed boundary 41

3.6. Mode shapes of the four span spring-mass system;
(a) Free-free system.

(b) Fixed-fixed system 42
3.7. Free vibrations of a four span spring-mass system of unsymmetric elements;
(a) Free-free boundary.
(b) Free-fixed boundary.
(c) Fixed-free boundary.
(d) Fixed-fixed boundary 43
3.8. Forced responses of symmetric spring-mass systems .. 45
3.9. Resonance curves of four span spring-mass systems;
(a) Free-free four-span system.
(b) Free-fixed four-span system 47
(c) Fixed-fixed four-span system.
(d) Infinite system 48
3.10. Propagation constant for a Bernoulli-Euler beam resting on knife-edge supports 53
4.1. Uniform beams resting on equi-spaced supports;
(a) Knife-edge supports.
(b) Spring supports 57
4.2. Free vibrations of the uniform beams on knife-edge supports;
(a) Hinged-hinged boundary.
(b) Clamped-clamped boundary 67
4.3. Propagation constant with $k_2=0$ 68
4.4. Propagation constant with $k_2=1$ 69
4.5. Propagation constant with $k_2=100$ 70
4.6. Normal modes of the four span Timoshenko beam on knife-edge supports 72

4.7. Free vibration of the beams on spring supports;
(a) Hinged-hinged boundary.
(b) Clamped-clamped boundary 73
4.8. Normal modes of the four span Timoshenko beam on spring supports 75
4.9. Forced vibration of the uniform beams on knife-edge supports;
(a) Four-span hinged-hinged beam
(b) Infinite-infinite beam 76
4.10. Resonance curves of four-span hinged beams;
(a) $k_2 = 0$ 77
(b) $k_2 = 1$ 78
(c) $k_2 = 100$ 79
4.11. Resonance curves of infinite beams on knife-edge supports;
(a) $k_2 = 0$ 80
(b) $k_2 = 1$ 81
(c) $k_2 = 100$ 82
4.12. Forced vibration of the uniform beams on spring supports;
(a) Four span beam with hinged ends.
(b) Infinite beam 83
4.13. Resonance curves for a four span hinged-hinged beams on spring supports;
(a) $k_1 = 0$ 84
(b) $k_1 = 0.5$ 85
4.14. Resonance curves for an infinite beam on spring

supports;

(a) $k_1 = 0$ 86

(b) $k_1 = 0.5$ 87

4.15. Timoshenko beam element for the Finite Element Method;

(a) Element division.

(b) Craggs' element showing the nodal displacements . 88

4.16. Propagation constant by the Finite Element Method;

(a) r = 0.04 91

(b) r = 0.08 92

4.17. Effect of rotary inertia and shear deformation on the natural frequencies of hinged beams

(a) Single span beam

(b) Four span beam. 99

4.18. Comparison of the computing time used 103

List of Tables

Table page

3.1. Natural frequencies of four span spring-mass systems of symmetric elements 41

3.2. Natural frequencies of four span spring-mass systems of unsymmetric elements 43

4.1. Natural frequencies of a four span beam on knife-edge supports;

(a) $k_2 = 0.$

(b) $k_2 = 1.$

(c) $k_2 = 100$ 71

4.2. Natural frequencies of a four span beam on spring supports;

(a) $k_1 = 0.$

(b) $k_1 = 0.5.$

(c) $k_1 = 50$ 74

4.3. Errors of Finite Element results for the four span Timoshenko beam on knife-edge supports;

(a) $r = 0.04.$

(b) $r = 0.08$ 93

Nomenclature

A cross-sectional area

b nondimensional frequency parameter

C,D arbitrary coefficients appearing in normal functions

E Young's modulus

G shear modulus

I moment of inertia

k spring constant

k' shape factor

l length of an individual periodic element

M nondimensional bending moment

m mass of a spring-mass oscillating system

N number of bays (spans or elements)

n number of intercoupling coordinates

p argument of hyperbolic normal functions

q argument of trigonometric normal functions

r slenderness ratio, $r^2 = I/Al^2$

s nondimensional parameter, $s^2 = EI/k'GAl^2$

V nondimensional shear force

x longitudinal coordinate

Y nondimensional amplitude of deflection

y total deflection of a beam

α,β nondimensional constants

λ eigenvalues of a transfer matrix

μ propagation constant

ξ nondimensional x-coordinate

ρ density of beam material

Ψ amplitude of the bending slope

ψ bending slope of the beam

ω rotational frequency

Matrices and Vectors

{C} coefficients appearing in normal modes

{d} generalized displacements

{f} generalized forces

[I] identity matrix

[K] stiffness matrix

[M] mass matrix

[S] transform matrix consisting of eigenvectors

[T] transfer matrix

{v} state vector

{w} vector of excitation

[Z] impedance matrix

[Λ] diagonal matrix of eigenvalues

Subscripts

i,j counting indices

L,R left and right boundary of an element

0,N left and right boundary of the whole system

I. INTRODUCTION AND LITERATURE SURVEY

A. Periodic Structure

Many practical structures are constructed in the form of a "periodic structure" mainly for appearance and lower building costs. The interior of a periodic structure consists of identical substructures connected in identical ways. Figure 1.1 shows two simplified examples of periodic structures. In the first example of a simple periodic structure, the identical periodic unit simply repeats over and over again, while the periodic unit in the second example is itself a periodic structure composed of periodic subunits. Being the generalization of the simple periodic structure, the latter is called a compound periodic structure. The constructions of bridges, ships and airplanes contain numerous examples of the second type, while railroad tracks, shafts with bearings and discs can be considered good examples of the first type.

For vibration analysis, these beam and plate-like structures with regularly spaced supports or stiffeners are often approximated by a uniform beam model resting on equi-spaced supports, known as a 'periodic beam'. These supports provide translational and rotational restraints to the flexural motion and thus may be represented by knife-edges or by translational and rotational elastic springs.

Being a mono-coupled system, the uniform beam resting on uniformly spaced knife-edge supports is one of the simplest case of the periodic structure, and hence it has been the favorite subject of earlier studies by Miles[16], Ayre and Jacobsen [1] and many others. Using a graphical technique of building up a nomograph of natural frequencies vs number of spans, it was shown in [1] that the natural frequencies of the multi-span beam can be obtained for two types of extreme boundaries, namely, simple and clamped. The repetitive nature of the groups of natural frequencies, as many frequencies in each group as there are spans, was observed in his study. A difference equation method was also shown to be applicable to find the natural frequencies of such beams [16]. However, this uniform beam model resting on knife-edge supports can not satisfactorily approximate many complicated types of periodically stiffened structures commonly used in aeronautical and naval frameworks.

B. Transfer Matrix

When the continuous beam is on uniformly spaced elastic springs which provide for constraints to the deflection and rotation of the beam the system becomes multi-coupled and requires matrix representation of coupling displacements and forces. For this type of problem the transfer matrix which relates such coupling displacements and forces in successive substructures was efficiently used by Lin[10] to analyze

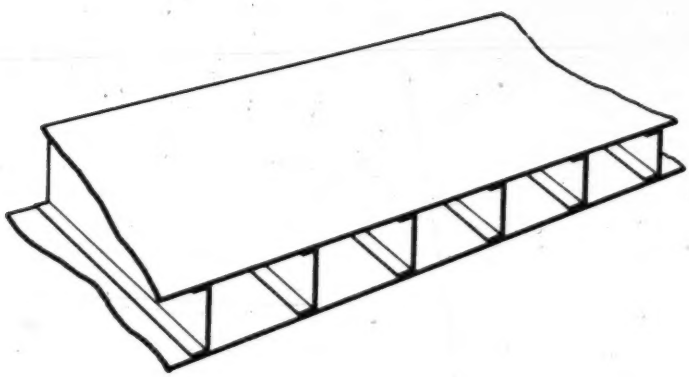

(a) A simple periodic structure.

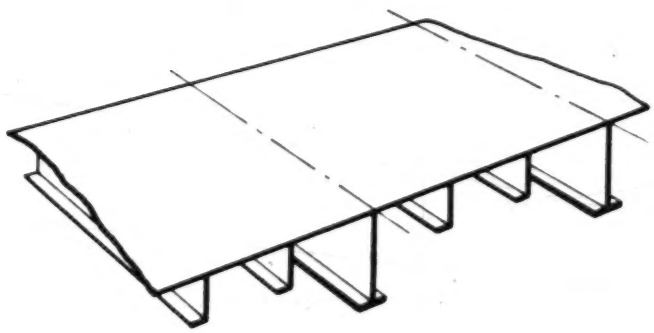

(b) A compound periodic structure.

Figure 1.1. Examples of periodic structures.

forced response of such periodic beams. Natural frequencies and principal modes were also found for periodic beams with certain extreme ends by Denke et al[5]. The transfer matrix method was shown to be suitable for the vibration analysis of such multi-span beams, as the extreme boundary conditions can be easily taken into account with the matrix equation. In addition, by working with a smaller sized matrix representing a single periodic beam element the computational effort becomes virtually independent of the number of spans. For years the transfer matrix method has been the major tool for vibration analysis of periodic beams. Tables of analytical transfer matrices for commonly appearing periodic beam elements are listed in [18].

C. Propagation Constant

When a periodic structure contains many supports, so many modes must be included in the analysis that the classical normal mode or transfer matrix methods become very cumbersome. Under this circumstance, it is convenient to regard the structure as being infinite in extent. Discrete principal modes do not exist for infinite systems, instead the differential equations governing linear vibration of the system yield free flexural waves which attenuate or propagate in the absence of damping and external forces. With some damping present, the forced response of a finite structure even with a few spans can be approximately obtained by assuming the number of spans being infinite and

by using the wave approach. This method, still giving acceptable results, would require far less computation.

When a periodic structure is vibrating in one of its free waves, there exists a constant ratio between the amplitude of motions in the adjacent periodic elements [3]. The natural log of this ratio of the amplitudes was first called the "propagation constant" by Heckl[6]. The flexural waves are then expressed as continuous functions of directional propagation constants.

In the works of Mead[11,12,13] and Sen Gupta[19,20] the propagation of the flexural waves in uniform beams were extensively investigated by the use of the propagation constant. The propagation constant in their works was obtained from the receptances of beam elements [2] and it was shown that the forced response of infinite beams are easily obtained by this propagation constant method. Even in the case of beams of finite number of spans they also managed to express some boundary conditions in terms of propagation constants. The mono-coupled system of a uniform beam on knife-edge supports was reconsidered by Sen Gupta[20] and it was shown that the natural frequencies are graphically obtainable from the curve of propagation constants. However, in the case of multi-coupled systems the representation of the extreme boundary condition in terms of propagation constant causes considerable difficulty [13] and hence the propagation constant method is hardly used in finding the natural frequencies of finite span beams

on other than knife-edge supports.

In the present study the propagation constant is recognized as the natural log of an eigenvalue of the transfer matrix. By doing so, the useful features of the propagation constant are still retained thus expanding the limit of the transfer matrix method.

D. Finite Element Method

The transfer matrix and the propagation constant methods have been based on the analytical expression of the normal mode solutions to the differential equations of beam vibration. Since these analytical solutions are restricted to only simple beam shapes so are the transfer matrix and the propagation constant methods.

Often periodic structures in engineering are so complex that a uniform beam model no longer represents the practical structure satisfactorily and therefore a numerical technique such as the Finite Element Method is required to analyze the dynamics of the realistic models of these complex periodic structures. In fact, almost any shape of structure, periodic or non-periodic, can be analyzed by this numerical technique with the aid of digital computers. However, as the number of spans increases the accuracy of the numerical results deteriorates while the computational costs grow enormously showing the limit of the application of straight numerical methods for the vibration analysis of periodic structures. Due to such limitations of the straight

numerical methods the transfer matrix method has gained renewed interest for the vibration analysis of periodic structures.

In the works of Orris and Petyt [17] the method of obtaining the propagation constant from the impedance matrix formulated by Finite Element Method was discussed. Independently, Meirovitch and Engels[14,15] showed that a matrix equation can be formed from the same impedance matrix using the so called Z-transform method. Again, by defining the propagation constant as the logarithmn of the eigenvalue of the transfer matrix, these two seemingly different techniques can be combined with added convenience resulting from the properties of the impedance matrix.

The transfer matrix method employed in the present study is different from the classical one in that the expression is derived from the impedance matrix resulting from the Finite Element Method not from the normal mode solution to differential equations. Thus the transfer matrix for a substructure is obtainable no matter how complex it may be. The analytical expression for the transfer matrix is also possible as a special case if the impedance matrix is expressed in terms of the normal mode solutions of the beam differential equations. The analytical expression for the propagation constant is then obtained from the eigenvalues of the analytically derived transfer matrix.

E. Timoshenko Beam

All the analytical studies of the flexural motions of elastic beams resting on multiple supports have been based on the Bernoulli-Euler beam theory neglecting the effect of rotary inertia and shear deformations. Corrections to the Bernoulli-Euler beam theory were given by Timoshenko[21] in which the governing differential equation includes the effect of rotary inertia and shear deformation. Huang[7] solved this differential equation by forming the normal mode equations for six common types of single span beams and discussed the effect of cross-sectional dimensions on the natural frequencies of a single span beam. However, little work has been done for the Timoshenko beam with intermediate supports. This prompted the choice of a multi-span Timoshenko beam as the numerical example for the present study.

Quite recently several Finite Element models have been proposed for the same Timoshenko beam as considered by Huang. Kapur's[8] and Craggs'[4] elements are two of these that have given good results over a wide range of cross-sectional parameters. These Finite Element analyses as well as Huang's analytical study of the beam vibration show that when solutions are based on the Bernoulli-Euler beam theory there are considerable differences except in the low frequency range of a long slender beam where the cross-sectional dimension is negligible with respect to the span length.

In this study the results are obtained analytically as well as numerically for the Timoshenko beam on multi-supports. These results are then compared with those based on Bernoulli-Euler beam theory in order to investigate the effect of cross-sectional dimensions on the natural frequencies of such beams. By simply setting the slenderness ratio to zero the present method is shown to yield the same results as those of Miles[16], Ayre and Jacobsen[1] and Lin[9].

II. TRANSFER MATRIX AND PROPAGATION CONSTANT

A. Introduction

When a periodic structure is approximated as a uniform beam on multiple supports, the transfer matrix can be easily formulated from the analytical solutions [9,10] or listed in [18]. However, many engineering structures are often of the form which may not be approximated as a uniform beam, and can only be analysed by a numerical technique such as the Finite Element Method. This requires a more general method of deriving the transfer matrix for any type of periodic structure.

In the following section the transfer matrix which relates the state vectors at two successive nodes is derived from the impedance matrix commonly formulated by the Finite Element Method. The impedance matrix of a single periodic unit relates the intercoupling generalized forces to the generalized displacements at both ends of the substructure. This impedance matrix, expressed either analytically or numerically, displays a general pattern - symmetry is one of the features. Formulated in terms of submatrices of the impedance matrix, the transfer matrix not only possesses all the properties of the classical transfer matrix, but also contains some added features resulting from the properties of the impedance matrix. For this reason simple manipulations, for example inversion, of the transfer matrix is possible. As in the case of beams supported on

equi-spaced elastic springs, the change of configuration of the periodic support can be easily done by simply adding or subtracting the appropriate terms to the diagonal elements of the impedance matrix.

Once the transfer matrix is formulated and its eigenvalues are found, the propagation constants are obtained as the natural logarithmns of these eigenvalues. In this way many properties of the propagation constant are simply interpreted by the algebraic properties resulting from the transfer matrix and its eigenvalues. All the considerations of the behavior of transfer matrices and their eigenvalues can be interpreted as those of propagation constants and vice versa. Therefore, only a brief discussion of the propagation constant is needed in this chapter.

For the vibration analysis of multi-unit periodic structures, either free or forced, often the multiplication of the element transfer matrix derived for a single substructure is required in order to find the total transfer matrix relating the state vectors from one end to another of the whole structure. This direct multiplication is satisfactory when the number of spans is small, however, for periodic structures composed of many substructures this direct multiplication would be very costly yielding doubtful results. In this circumstance, either the Cayley-Hamilton theorem or the similarity transform method can be used so that the accuracy of the numerical results improve while

reducing the computational efforts.

In some cases only the propagation constants (or the eigenvalues of the transfer matrix) are needed instead of the transfer matrix itself. Since the transfer matrix is expressed in terms of submatrices of the impedance matrix, the eigenvalues of the transfer matrix or the propagation constant can be related directly to the impedance matrix. In this way much of the computational effort is reduced by eliminating the formulation procedure of the transfer matrix.

B. Transfer Matrix from Impedance Matrix

Consider a periodic system shown in Figure 2.1, and suppose that the impedance matrix [Z] for the subsystem

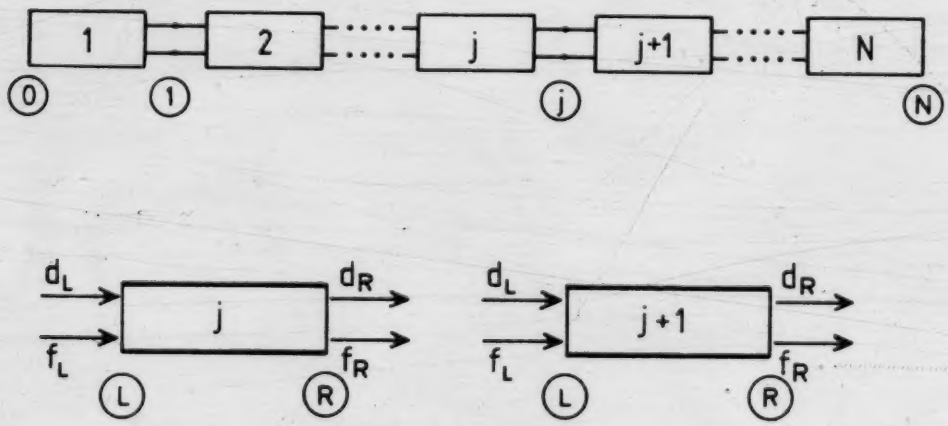

Figure 2.1. Block diagram of a periodic structure showing the generalized displacements and forces.

shown in Figure 2.1 is formed as

$$\{f\} = [Z]\{d\} \tag{2.1}$$

where {d} and {f} denote the generalized displacement and force vectors, respectively. The impedance matrix, [Z] is of the familiar form

$$[Z] = [K]-\omega^2[M] \tag{2.2}$$

when formulated by the Finite Element Method. Here, [K] and [M] denote the stiffness and mass matrices, respectively. This impedance matrix as well as the displacement and force vectors can be partitioned as

$$\begin{Bmatrix} f_L \\ f_R \end{Bmatrix}_j = \begin{bmatrix} Z_{LL} & Z_{LR} \\ Z_{RL} & Z_{RR} \end{bmatrix} \begin{Bmatrix} d_L \\ d_R \end{Bmatrix}_j \tag{2.3}$$

where the subscripts *L* and *R* denote the left and right ends of the subsystem. In equation (2.3), it is assumed that the internal nodal degrees of freedom are already removed, if necessary, by the procedure described in [14].

It can be easily shown that the equation (2.3) can be rearranged in the form

$$\begin{Bmatrix} d_R \\ f_R \end{Bmatrix}_j = \begin{bmatrix} -Z_{LR}^{-1}Z_{LL} & Z_{LR}^{-1} \\ -Z_{RR}Z_{LR}^{-1}Z_{LL}+Z_{RL} & Z_{RR}Z_{LR}^{-1} \end{bmatrix} \begin{Bmatrix} d_L \\ f_L \end{Bmatrix}_j. \tag{2.4}$$

But,

$$\{d_R\}_j = \{d_L\}_{j+1} \tag{2.5}$$

by the compatibility relationship of displacements and

$$\{f_R\}_j = -\{f_L\}_{j+1} \tag{2.6}$$

by the equilibrium condition when there are no external forces applied.

Equations (2.5) and (2.6) are substituted back into equation (2.4) to yield a matrix difference equation relating generalized displacements and forces in the successive subsystems *j* and *j+1* as

$$\begin{Bmatrix} d_R \\ f_R \end{Bmatrix}_{j+1} = [T] \begin{Bmatrix} d_L \\ f_L \end{Bmatrix}_j . \tag{2.7}$$

[T] denotes the transfer matrix by definition consisting of submatrices as

$$[T] = \begin{bmatrix} -Z_{LR}^{-1} Z_{LL} & Z_{LR}^{-1} \\ Z_{RR} Z_{LR}^{-1} Z_{LL} - Z_{RL} & -Z_{RR} Z_{LR}^{-1} \end{bmatrix} . \tag{2.8}$$

The augmented vector of generalized displacements and forces is called the state vector at a node.

C. Properties of Transfer Matrix

Inversion

It can be noted that the equation (2.3) may be rearranged in the different order from equation (2.4) as

$$\begin{Bmatrix} d_L \\ f_L \end{Bmatrix}_j = \begin{bmatrix} -Z_{\bar{R}L}' Z_{RR} & Z_{\bar{R}L}' \\ -Z_{LL} Z_{\bar{R}L}' Z_{RR} + Z_{LR} & Z_{LL} Z_{\bar{R}L}' \end{bmatrix} \begin{Bmatrix} d_R \\ f_R \end{Bmatrix}_j . \tag{2.9}$$

Substitution of equations (2.5) and (2.6) into equation (2.9) yields a transfer matrix in the opposite direction to equation (2.8), i.e., the inverse of the transfer matrix, [T] as defined in equation (2.8).

$$\begin{Bmatrix} d_L \\ f_L \end{Bmatrix}_j = [T^{-1}] \begin{Bmatrix} d_R \\ f_R \end{Bmatrix}_{j+1} . \tag{2.10}$$

Thus the inverse of transfer matrix, $[T^{-1}]$ is another transfer matrix which consists of the submatrices as

$$[T^{-1}] = \begin{bmatrix} -Z_{\bar{R}L}' Z_{RR} & -Z_{\bar{R}L}' \\ -Z_{LL} Z_{\bar{R}L}' Z_{RR} + Z_{LR} & -Z_{LL} Z_{\bar{R}L}' \end{bmatrix} . \tag{2.11}$$

Direct multiplication of [T] and $[T^{-1}]$ in equations (2.8) and (2.11) confirms an identity matrix, i.e.,

$$[T][T^{-1}] = [I] . \tag{2.12}$$

This derivation of $[T^{-1}]$ expressed by equation (2.11) does not require any additional calculations. If the transpose of $[T^{-1}]$ is taken as

$$[T^{-T}] = \begin{bmatrix} -Z_{RR}^{T} Z_{RL}^{-T} & Z_{LR}^{T} - Z_{RR}^{T} Z_{RL}^{-T} Z_{LL}^{T} \\ -Z_{RL}^{-T} & -Z_{RL}^{-T} Z_{LL}^{T} \end{bmatrix} \tag{2.13}$$

and noting that the impedance matrix [Z] is symmetric, i.e.,

$$Z_{LL}^{T} = Z_{LL},\ Z_{RR}^{T} = Z_{RR} \text{ and } Z_{RL}^{T} = Z_{LR}. \tag{2.14}$$

then the equation (2.13) can be simplified as

$$[T^{-T}] = \begin{bmatrix} -Z_{RR} Z_{LR}^{-1} & Z_{RL} - Z_{RR} Z_{LR}^{-1} Z_{LL} \\ -Z_{LR}^{-1} & -Z_{LR}^{-1} Z_{LL} \end{bmatrix}. \tag{2.15}$$

Comparison of equation (2.15) with equation (2.8) immediately suggests an algorithm for inversion of the transfer matrix which is expressed by equation (2.8):

(a) Partition the transfer matrix into four submatrices,

(b) Switch the left top and right bottom submatrices,

(c) Change the sign of right top and left bottom submatrices,

(d) Take the transpose of the matrix obtained in (c).

Eigenvalues and Eigenvectors

Assuming that a constant ratio (eigenvalue), λ exists such that

$$\{d_R\} = \lambda\{d_L\}, \tag{2.16}$$

and

$$\{f_R\} = -\lambda\{f_L\}, \tag{2.17}$$

and by subsituting equations (2.16) and (2.17) for $\{d_R\}$ and $\{f_R\}$, matrix equation (2.3) can be rewritten as

$$\{f_L\} = [Z_{LL}]\{d_L\} + \lambda[Z_{LR}]\{d_L\} \tag{2.18a}$$

$$-\lambda\{f_L\} = [Z_{RL}]\{d_L\} + \lambda[Z_{RR}]\{d_L\}. \tag{2.18b}$$

Equation (2.18a) is multiplied by λ, then added to equation (2.18b) to yield

$$[\lambda^2 Z_{LR}+\lambda(Z_{LL}+Z_{RR})+Z_{RL}]\ \{d_L\} = 0. \tag{2.19}$$

Equation (2.19) does not have an immediate solution for λ, except when it is a scalar equation. However, together with a trivial relationship

$$\{\lambda d_L\} = \lambda\{d_L\} \tag{2.20}$$

equation (2.19) may be augmented as

$$\begin{bmatrix} 0 & Z_{LR} \\ Z_{RL} & Z_{LL}+Z_{RR} \end{bmatrix} \begin{Bmatrix} d_L \\ \lambda d_L \end{Bmatrix} = \lambda \begin{bmatrix} Z_{LR} & 0 \\ 0 & -Z_{LR} \end{bmatrix} \begin{Bmatrix} d_L \\ \lambda d_L \end{Bmatrix}. \qquad (2.21)$$

Equation (2.21) is of the same size as the transfer matrix, [T] and allows the use of ordinary eigenvalue subroutines to find λ values and the corresponding eigenvectors $\{d_L\}$. The generalized force vector, $\{f_L\}$ is then found by the relationship

$$\{f_L\} = [Z_{LL}]\{d_L\} + [Z_{LR}]\{\lambda d_L\}. \qquad (2.22)$$

The augmented vector of $\{d_L\}$ and $\{f_L\}$ obtained from equations (2.21) and (2.22) is the eigenvector of the transfer matrix.

It can be easily shown that the transfer matrix and its inverse possess an identical characteristic equation and thus the same set of eigenvalues. It follows then that the eigenvalues of the transfer matrix must be pairwise reciprocals.

Multiplication of transfer matrices

According to the Cayley-Hamilton theorem, a matrix itself satisfies its own characteristic equation and thus the power of a matrix of size *2n* may be expressed by a linear combination of any *2n* linearly independent

polynomials of the matrix,

$$[T^N] = \sum_{j=1}^{n} [c_j T^j + d_j T^{-j}]. \qquad (2.23)$$

This equation must be satisfied by the inverse of [T] as well

$$[T^{-N}] = \sum_{j=1}^{n} [c_j T^{-j} + d_j T^j]. \qquad (2.24)$$

Addition and subtraction of equations (2.23) and (2.24) yield

$$[T^N+T^{-N}] = \sum_{j=1}^{n} a_j [T^j+T^{-j}] \qquad (2.25a)$$

$$[T^N-T^{-N}] = \sum_{j=1}^{n} b_j [T^j-T^{-j}] \qquad (2.25b)$$

where n denotes half the size of the transfer matrix. The constants a_j and b_j are determined by substituting the eigenvalues λ for [T] in equations (2.25a) and (2.25b). The N-th power of the transfer matrix, $[T^N]$ is then obtained from

$$[T^N] = \sum_{j=1}^{n} a_j [T^j+T^{-j}] + \sum_{j=1}^{n} b_j [T^j-T^{-j}] \qquad (2.26)$$

It is often more convenient to find $[T^N]$ by the so-called similarity transform method. Since the transfer matrix has $2n$ linearly independent eigenvectors it can be diagonalized as

$$[T] = [S][\Lambda][S^{-1}] \tag{2.27}$$

where the columns of the matrix, [S] are the eigenvectors of [T] and [Λ] is a diagonal matrix with the corresponding eigenvalues of [T] along its diagonal. Then the multiplication of [T] can be done as

$$[T^N] = [S][\Lambda^N][S^{-1}]. \tag{2.28}$$

D. Propagation Constants and Transfer Matrix

Although the concept of the propagation constant was originally developed in wave theory [6], independent of the transfer matrix, it is quite clear that there exists a definite relationship between them. By definition

$$\begin{aligned} \{v\}_{j+1} &= [T]\{v\}_j \text{ : transfer matrix} \\ \{v\}_{j+1} &= \exp(\mu)\{v\}_j \text{ : propagation constant} \end{aligned} \tag{2.29}$$

where {v} denotes the state vector consisting of the generalized displacements and forces as shown in equation (2.8), and μ is called the propagation constant.

The latter can be subtracted from the former in equation (2.29) to yield

$$[T - \exp(\mu)I]\ \{v\}_j = 0. \tag{2.30}$$

Thus the propagation constant, μ may be understood as the natural logarithmns of the eigenvalues of the transfer matrix. Hence the propagation constant in this study does not require a separate formulation, but is evaluated from the transfer matrix and its eigenvalues.

The propagation constants as well as the eigenvalues of the transfer matrix are generally complex numbers. Since the eigenvalues of the transfer matrix are pairs of reciprocals, the propagation constants are pairs of opposite signs.

For the transfer matrix of size $2n$, there exist n pairs of propagation constants and hence for a mono-coupled system only a single curve is needed to show the propagation constant.

E. Discussion

The transfer matrix obtained from the impedance matrix as in the present study can be applied to any complex periodic structure since the impedance matrix can be always formed by the Finite Element Method. The Finite Element Method commonly uses polynomial interpolation functions, for instance, a cubic function is normally assumed for the deflection of beams. The accuracy of the Finite Element Method depends mainly on how closely these interpolation functions approximate the exact normal modes. If these interpolation functions happen to be identical to the normal modes, the Finite Element Method yields the exact solution

within the round-off error due to the digital computation. In the case of a uniform beam the analytical expression for the transfer matrix can be obtained through the procedure as described in the section II.B, from the impedance matrix analytically formulated using the two hyperbolic and trigonometric normal modes as the interpolation functions.

The cross-symmetric property of the transfer matrix has been considered quite important in the earlier studies [9,10]. This cross-symmetry of a transfer matrix is expressed in the indicial form as

$$t_{i,j} = t_{2n+1-j,\,2n+1-i} \tag{2.31}$$

where $t_{i,j}$ is the i-th row and j-th column entry of the transfer matrix of size $2n$. This cross-symmetry together with other properties of the transfer matrix leads to an algorithm for transfer matrix inversion as

$$\bar{t}_{i,j} = (-1)^{i+j}\, t_{i,j} \tag{2.32}$$

where $\bar{t}_{i,j}$ is the i-th row and j-th column entry of $[T^{-1}]$.

When the periodic unit is symmetric about its center it is possible to obtain a cross-symmetric transfer matrix by a suitable choice of the order and sign convention for the components of the state vector. However, the transfer matrices are not generally cross-symmetric, and even so, the proper reordering and rearranging of a transfer matrix into

a cross-symmetric form, especially with the digital computer is extremely difficult. In the present study dealing with the generally shaped periodic structures, the use of equation (2.32) can not be made and thus a new algorithm of inversion which does not require the cross-symmetry be developed as in the section II.C.

Certainly the eigenvalues and eigenvectors can be found by ordinary subroutines directly from the transfer matrix. When its application is restricted to the periodic beams (the size of the transfer matrix is at most four) it matters little how the eigenvalues are obtained. However, it is possible to greatly reduce the computational effort for finding the eigenvalues and eigenvectors by using the submatrices of the impedance matrix instead of the transfer matrix as described in equations (2.16) through (2.22). When the periodic unit is symmetric further reduction of computation is possible by halving the size of matrix involved [14,15]. This is possible because of the special pattern of the impedance matrix of the symmetric subsystem, although it was not pointed out in his study. By halving the size of matrix for the eigenvalue subroutine the computational cost is reduced by a factor of approximately eight.

By expressing the transfer matrix in terms of the submatrices of the impedance matrix it can be easily shown that the transfer matrix and its inverse possess the same characteristic equation and thus the same set of

eigenvalues. Consequently, the determinant of a transfer matrix is always unity and the eigenvalues of the transfer matrix are therefore pairwise reciprocals. This leads to the conclusion that the propagation constants which are defined as the logarithmns of the eigenvalues must be pairs of opposite signs. Physically this should be true since nature would not recognize the negative and positive directions of the structure.

Without excitation, a wave signal is not amplified as it propagates along the structure. This implies that an eigenvalue whose magnitude is greater than unity corresponds to a negative going wave and its reciprocal to a positive going wave. In terms of propagation constants, the one with a positive real part corresponds to a negative going wave while the one with a negative real part to a postive going wave.

Generally, the propagation constant as well as an eigenvalue of the transfer matrix is a complex number. The real part of the propagation constant represents the amplitude decay; the imaginary part the phase difference at two successive nodes. An energy carrying free flexural wave is possible in the distinct frequency zones where the real part of propagation constant vanishes. For a finite structure the wave motion satisfies the extreme end conditions only at the certain groups of discrete values of frequencies within these propagation zones. These groups of frequencies constitute the natural frequencies of the whole

structure, which will be discussed in the next chapter.

In order to use the transfer matrix for the vibration analysis of the *N*-span periodic structure, free or forced, the first step required may be the multiplication of the element transfer matrix. Three different techniques are suggested, namely; direct multiplication, application of Cayley-Hamilton theorem and the similarity transform method. Direct multiplication is of course the simplest and can be satisfactorily used for a structure with a few spans (three or four spans at the most). This direct multiplication is the only available technique in the case where the structure is composed of different substructures. Considering that the matrix multiplication is a costly process losing the accuracy of the numerical results, this direct multiplication can not be used for a periodic structure of many spans.

The use of the Cayley-Hamilton theorem also contains the direct multiplication $2n$ times (n times for [T] and n times for $[T^{-1}]$). Because of this direct multiplication involved, this method is not suitable for multi-coupled systems when there are many coupling coordinates. For the sake of efficiency, the Cayley-Hamilton theorem for the multiplication of the transfer matrix is not directly applied to the transfer matrix itself, but to the sum and the difference of the transfer matrix and its inverse. In this way, the computation deals with two half-sized matrices instead of one double-sized and this would result in

reduction of the computational effort. Since the sum and the difference of the transfer matrix and its inverse are of a weakly coupled form, with half the components being equal to or close to zero, the accuracy of the results also improves.

On the other hand, the method of similarity transform does not require any multiplication. Instead, it requires that the eigenvectors of the transfer matrix be found to form the matrix [S] and its inverse, $[S^{-1}]$. The eigenvectors are automatically obtained in most eigenvalue subroutines, however, the inversion of [S] is again a costly process. Fortunately, many vibration problems do not need $[S^{-1}]$ to be found as it will be shown in the next chapter. In such cases the method of similarity transform can be most efficiently used.

III. HARMONIC MOTIONS OF PERIODIC STRUCTURES

A. Introduction

In the previous chapter a transfer matrix was formulated for a typical bay of a periodic structure. This element transfer matrix was then shown to be multiplied to represent a transfer matrix for an *N*-bay periodic structure, i.e.,

$$\{v\}_N = [T^N]\{v\}_0 \tag{3.1}$$

where $[T^N]$ denotes *N*-th power of a transfer matrix, $[T]$, and at the same time the total transfer matrix relating the state vectors at the ends of the periodic structure.

Generally speaking, the two end bays of a periodic structure are different from the typical internal bay due to the boundary conditions of the whole structure - see Figure 3.1(a). In this case the transfer matrix for the two end bays may be formulated separately and the transfer matrix for the whole system can be obtained as

$$\{v\}_N = [T] \, [T^{N-2}] \, [T]_1 \, \{v\}_0 \tag{3.2}$$

where $[T]_1$ and $[T]_N$ denote the transfer matrices for the first and last elements of the structure. Fortunately in many homogeneous boundary beam cases, the two end bays can be considered identical to the other interior bays. These

are the cases where the extreme boundaries offer more constraints than the intermediate supports - see Figure 3.1(b). The boundary condition is then applied to the state vectors $\{v\}_0$, $\{v\}_N$ in equation (3.1) to obtain the frequency equation of the complete system. Therefore, without loss of generality, it is assumed in the present study that $[T^N]$ represents the transfer matrix for the whole structure relating the state vectors $\{v\}_0$ and $\{v\}_N$.

Special consideration is given to mono-coupled systems where the periodic units are inter-coupled by a single displacement or a force (generalized). A spring-mass oscillating system and a uniform beam resting on knife-edge supports are the examples of a mono-coupled system. The transfer matrix for a mono-coupled system is of size two, and hence it has a pair of eigenvalues and consequently a pair of propagation constants. This propagation constant can be represented by a single curve and it is possible to use a graphical technique to find the natural frequencies of the system. In the case of a multi-coupled system, the set of frequency equations is of determinantal form, consisting of implicit functions of frequencies, which can be solved by an iterative technique or a numerical scheme which does not require explicit knowledge of frequencies.

While it is possible to consider transient or non-harmonic excitation problems, only the steady-state harmonic forced response problems are considered in this study. In such cases the response can be uniquely

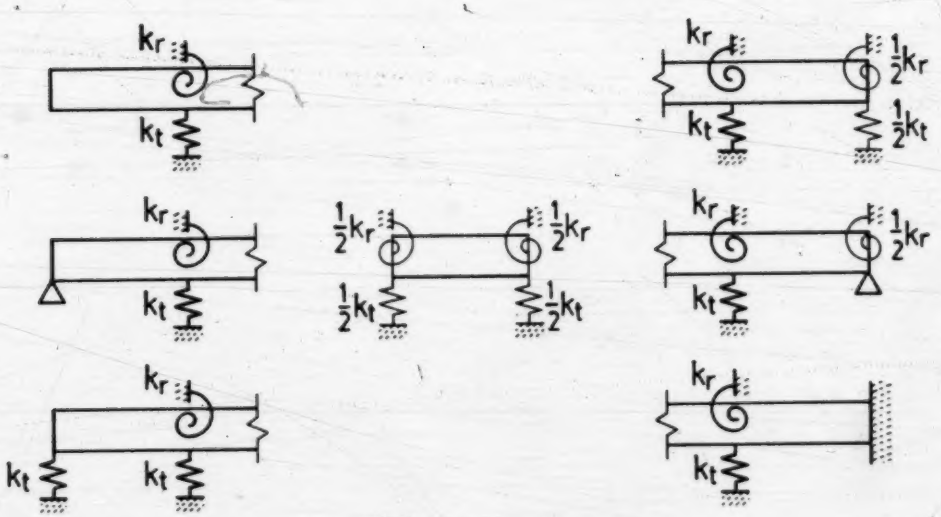

(a) End transfer matrices are required.

(b) End transfer matrices are not required.

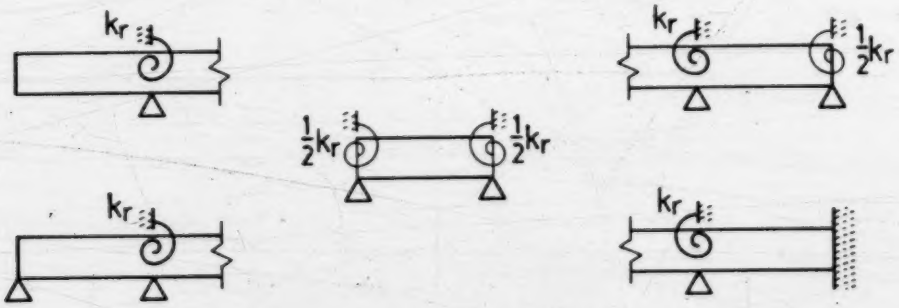

Figure 3.1. Uniform beams with end elements different from the periodic element.

determined without any iterative procedure.

When a periodic structure contains infinitely many spans the frequency equation is no longer obtained. However, the steady-state solutions to the harmonic excitation are still available from relatively simple calculations. When this response is shown in the form of a resonance curve the frequency at which the resonance occurs can be considered as the natural frequency of such an infinite system.

B. Natural Frequencies

Consider a periodic structure consisting of N periodic substructures with $2n$ degrees of freedom at each node. There exist $2n$ boundary conditions - n for the left boundary and n for the right. These boundary conditions are substituted into equation (3.1) and a set of equations for the boundary conditions is obtained. If the boundary condition is such that all the generalized displacements are zeros in the state vectors, $\{v\}_0$ and $\{v\}_N$ so that

$$[T_{1,\frac{N}{2}}] \{f\}_0 = 0 \qquad (3.3)$$

where $[T_{1,\frac{N}{2}}]$ denotes the top-right submatrix of $[T^N]$. Equation (3.3) represents a set of n homogeneous algebraic equations, which has nontrivial solutions if and only if the determinant of $[T_{1,\frac{N}{2}}]$ vanishes

$$\det[T_{12}^{N}] = 0. \tag{3.4}$$

The frequency equation can be obtained differently if the similarity transform method is used for obtaining $[T^N]$. From equation (2.28)

$$\{v\}_N = [S][\Lambda^N][S^{-1}]\{v\}_0. \tag{3.5}$$

Premultiplication of both sides by $[S^{-1}]$ yields

$$[S^{-1}]\{v\}_N = [\Lambda^N][S^{-1}]\{v\}_0. \tag{3.6}$$

By setting

$$[S]\{C\}_N = \{v\}_N, \tag{3.7}$$

and

$$[S]\{C\}_0 = \{v\}_0, \tag{3.8}$$

equation (3.5) can be rewritten as

$$\{C\}_N = [\Lambda^N]\{C\}_0. \tag{3.9}$$

In these equations $\{C\}_0$ and $\{C\}_N$ denote the arbitrary coefficients to be determined by the boundary conditions at the left and right ends of the structure. Applying the extreme boundary conditions to equations (3.7) and (3.8) a

set of $2n$ homogeneous frequency equations are obtained. If the both ends are fixed, i.e., all the generalized displacements are zeros, then

$$[S]_1 \{C\}_o = 0$$
$$[S\Lambda^N]_1 \{C\}_o = 0 \qquad (3.10)$$

where the subscript 1 in equation (3.10) denotes the upper half of the matrix and the total number of equations in (3.10) is $2n$. Boundary conditions other than fixed ends can be handled similarly. These frequency equations (3.4) or (3.10) are highly transcendental and not to be solved simply, because the components of the matrices $[T^N]$ and $[S]$ are implicit functions of frequencies. Thus a numerical algorithm which does not require explicit knowledge of the characteristic determinant is needed to solve the frequency equation. Meirovitch and Engels[15] suggested an algorithm which is referred to as Muller's method. For the detailed discussion for the Muller's method one should refer to [15].

C. Steady-state Harmonic Response

Consider again an N-bay structure and suppose that a harmonic excitation is introduced at the node j. The state vectors at the ends, $\{v\}_o$, and $\{v\}_N$ are now related as

$$\{v\}_N = [T^N]\{v\}_o + [T^{N-j}]\{w\}_j \qquad (3.11)$$

where $\{w\}_j$ is the input vector at j. Equation (3.11) contains total of $4n$ unknown quantities in $2n$ equations. Upon imposing $2n$ boundary conditions on $\{v\}_0$ and $\{v\}_N$, the number of total unknowns is reduced to $2n$, giving a set of $2n$ equations with $2n$ unknowns. This equation is inhomogeneous due to the input vector and thus the state vectors $\{v\}_0$ or $\{v\}_N$ can be uniquely determined. The response at the intermediate node, i then can be obtained by

$$\begin{aligned} \{v\}_i &= [T^i]\{v\}_0: \quad \text{if } i \le j, \\ \{v\}_i &= [T^i]\{v\}_0 + [T^{i-j}]\{w\}_j: \quad \text{if } i > j. \end{aligned} \tag{3.12}$$

In the case where the input vector is introduced in between the nodes a partial transfer matrix is needed, while the rest of the analysis is the same. Suppose an excitation is introduced at a point x in between the nodes $j-1$ and j, then the equation (3.11) can be modified as

$$\{v\}_N = [T^N]\{v\}_0 + [T^{N-j}][T_{j-x}]\{w\}_x \tag{3.13}$$

where $[T_{j-x}]$ denotes a partial transfer matrix transferring the input vector from the point x to the node j. When there are multiple input vectors the term due to other input vectors can be simply added to the RHS of equation (3.11).

The problem of the periodic structure consisting of infinitely many spans is not difficult to solve but needs separate consideration. Figure 3.2(a) shows an example of a

semi-infinite system. The boundary condition at the right end is that there is no wave returning from it so that half the coefficients $\{C\}_o$ in equations (3.7) and (3.8) which correspond to negative going waves are zeros. This gives n boundary conditions together with another n boundary conditions at the other end provide $2n$ required equations.

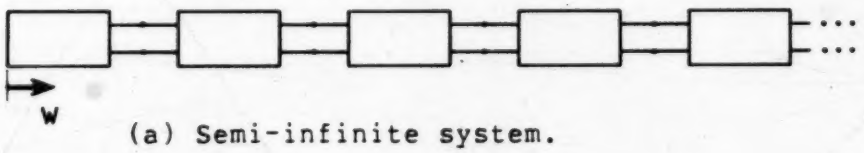

(a) Semi-infinite system.

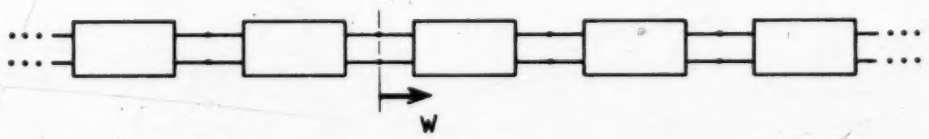

(b) Infinite-infinite system.

Figure 3.2. Harmonically excited infinite systems.

Consider an example of a semi-infinite system with the excitation at the free end. From equation (3.6)

$$\{v\}_o+\{w\}_o = [S]\{C\}_o \qquad (3.14)$$

where half the elements of $\{C\}_o$ which correspond to negative

going waves are zeros and the bottom half of $\{v\}_o$ are also zeros so that n equations from the bottom are solved first for the n nonzero coefficients then the response is given by the upper half of the equations. In the case of the infinite-infinite system with the exciting force introduced at the middle as shown in Figure 3.2(b), the additional n equations are the conditions at the excitation that the n generalized displacements are continuous.

D. Mono-coupled System

Figure 3.3 shows two examples of mono-coupled system. The 2x2 transfer matrix for a mono-coupled system is of the form

$$[T] = \begin{bmatrix} t_{11} & t_{12} \\ t_{21} & t_{22} \end{bmatrix}. \tag{3.15}$$

Since the determinantal value of a transfer matrix is always unity the inverse of [T] in equation (3.15) is simply

$$[T^{-1}] = \begin{bmatrix} t_{22} & -t_{12} \\ -t_{21} & t_{11} \end{bmatrix}. \tag{3.16}$$

Let the eigenvalues of [T] be λ and $1/\lambda$ and the propagation constant be $\pm\mu$, then the total transfer matrix, $[T^N]$ is obtained by the equations (2.25) and (2.26) as

$$[T^N] = \begin{bmatrix} \cosh N\mu + \frac{\sinh N\mu}{\sinh \mu}\cdot\frac{(t_{11}-t_{22})}{2} & \frac{\sinh N\mu}{\sinh \mu} t_{12} \\ \frac{\sinh N\mu}{\sinh \mu} t_{21} & \cosh N\mu - \frac{\sinh N\mu}{\sinh \mu}\cdot\frac{(t_{11}-t_{22})}{2} \end{bmatrix} \quad (3.17)$$

where it is noted that

$$\begin{aligned} \cosh\mu &= 0.5(\lambda+1/\lambda) \\ &= 0.5(t_{11}+t_{22}). \end{aligned} \quad (3.18)$$

(a) A spring-mass oscillating system.

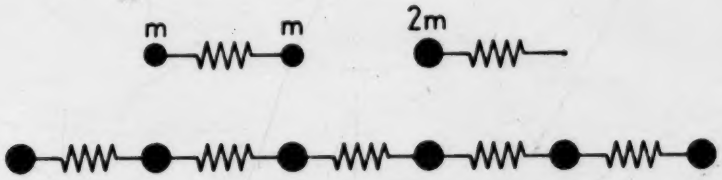

(b) A uniform beam on knife-edge supports.

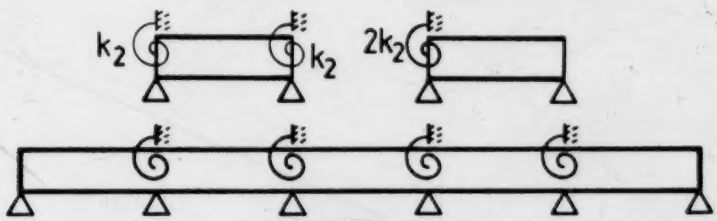

Figure 3.3. Examples of mono-coupled systems showing two possible element divisions.

In the special case where the periodic element is symmetric about its center, $t_{11}=t_{22}=\cosh\mu$, so that equation (3.17) can be simplified as

$$[T^N] = \begin{bmatrix} \cosh N\mu & \frac{\sinh N\mu}{\sinh\mu} t_{12} \\ \frac{\sinh N\mu}{\sinh\mu} t_{21} & \cosh N\mu \end{bmatrix}. \qquad (3.19)$$

Three different boundary conditions may be considered;

1) Both ends free

$$\sinh N\mu/\sinh\mu=0, \text{ or } \mu=j\pi i/N \ (j=1,2,\ldots,N-1) \quad \text{or } t_{21} = 0 \qquad (3.20)$$

2) Both ends fixed

$$\sinh N\mu/\sinh\mu=0, \text{ or } \mu=j\pi i/N \ (j=1,2,\ldots,N-1) \quad \text{or } t_{12} = 0 \qquad (3.21)$$

3) One end free, one end fixed

1. Symmetric element

$$\cosh N\mu=0, \text{ or } \mu=(j+0.5)\pi i/N \ (j=0,1,..,N-1) \qquad (3.22)$$

2. Unsymmetric element

$$\cosh N\mu \pm 0.5\sinh N\mu(t_{11}-t_{22})/\sinh\mu = 0. \qquad (3.23)$$

For the spring-mass oscillating system shown in Figure 3.3(a), the transfer matrix is obtained as - see Appendix A.1

$$[T] = \begin{bmatrix} 1-b^2 & -1 \\ b^2(2-b^2) & 1-b^2 \end{bmatrix}, \tag{3.24}$$

where $b^2=m\omega^2/k$. The propagation constant is obtained from this transfer matrix as

$$\mu = \cosh^{-1}(1-b^2) \tag{3.25}$$

which is shown in Figure 3.4. Above the frequency, $b=\sqrt{2}$ the wave attenuates with increasing amplitude decay as the frequency increases and the wave propagation is only possible in the frequency zone, $b\leq\sqrt{2}$, where the real part of the propagation constant vanishes. Within the propagation zone at the points numbered 1,2,..., where $\mu=j\pi i/N$ (N=4 in Figure 3.4), the natural frequencies of either the free-free or the fixed-fixed systems are read, i.e.,

$$b = \sqrt{1-\cos(j\pi/N)} \quad (j=1,2,..,N-1) \tag{3.26}$$

and additional roots exist

$$b = 0 \text{ and } \sqrt{2} \tag{3.27}$$

in the case of free-free boundary.

The natural frequencies of the system with the free-fixed boundaries fall at the middle of these points corresponding to the natural frequencies of the free-free or fixed-fixed systems as

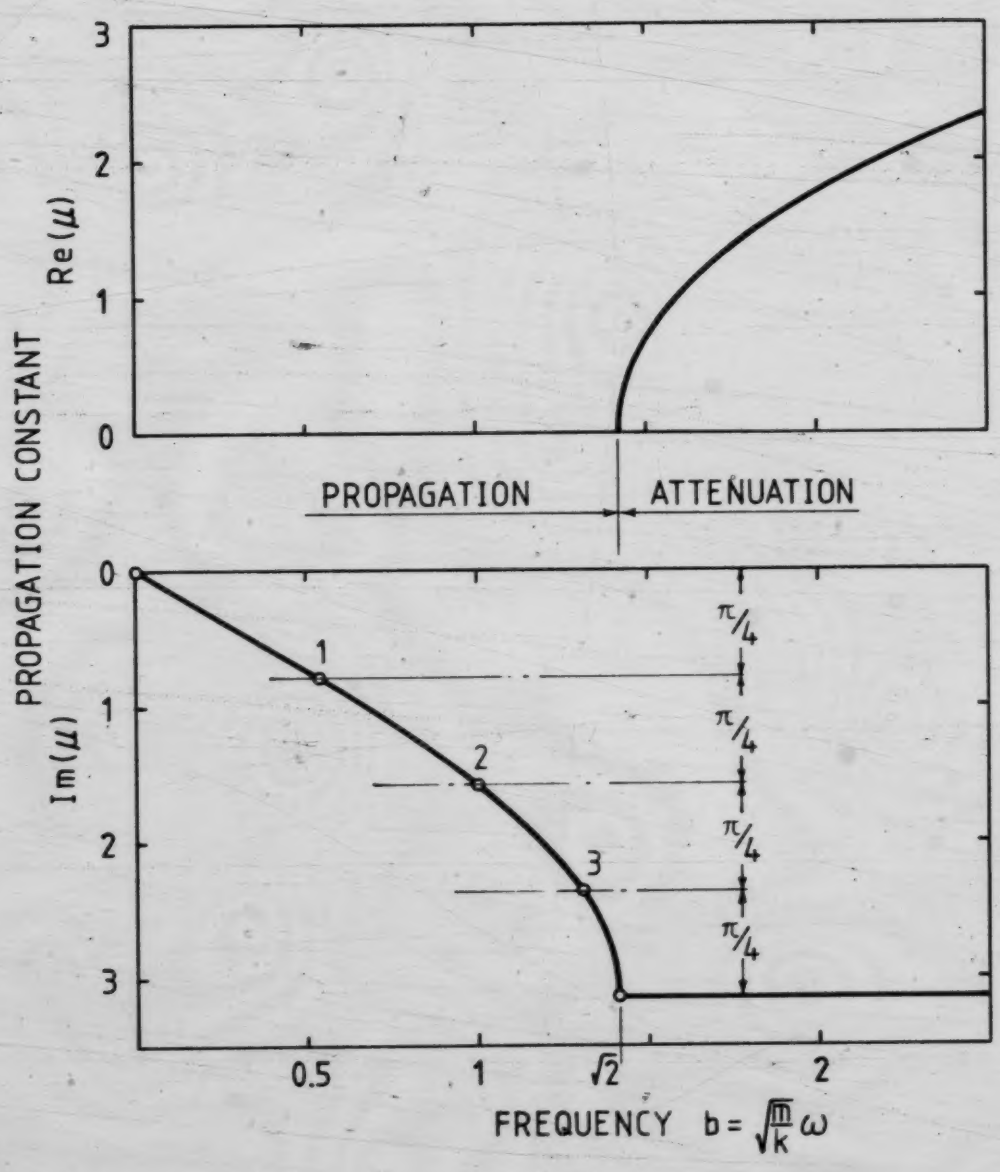

Figure 3.4. Propagation constant for a spring-mass system.

$$b = \sqrt{1-\cos((j+0.5\pi)/N)} \quad (j=0,1,2,..,N-1) \qquad (3.28)$$

only when the periodic element is symmetric. For the four span spring-mass systems of symmetric elements shown in Figure 3.5 the natural frequencies are obtained by this method and they are given in Table 3.1. The mode shapes corresponding to these natural frequencies of the free-free and fixed-fixed cases are shown in Figure 3.6. The axial motion of the mass is shown vertically in this figure.

The same spring-mass system can be divided into unsymmetric periodic elements as shown in Figure 3.3(a). The transfer matrix in this case becomes - see Appendix A.2

$$[T] = \begin{bmatrix} 1-2b^2 & -1 \\ 2b^2 & 1 \end{bmatrix}. \qquad (3.29)$$

The propagation constant is identically obtained as in equation (3.25) and Figure 3.4. Figure 3.7 shows the four span spring-mass systems of unsymmetric elements. Note that the mass at the ends becomes $2m$ in this case. The natural frequencies of the symmetric boundary systems, (a) free-free and (d) fixed-fixed, may be determined graphically from the propagation constant curve as in the case of symmetric element systems. Whereas, those of the unsymmetric boundary systems, (b) free-fixed and (c) fixed-free, can be obtained by solving the frequency equation (3.23). These results are given in Table 3.2.

Table 3.1. Natural frequencies of four span spring-mass systems of symmetric elements. ($b=\sqrt{\frac{m}{k}}\omega$)

No. MODE	FREE-FREE	FREE-FIXED	FIXED-FIXED
1	0.0	0.276	0.541
2	0.541	0.786	1.0
3	1.0	1.176	1.307
4	1.307	1.387	
5	1.414		

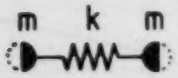

(a) Free-free boundary.

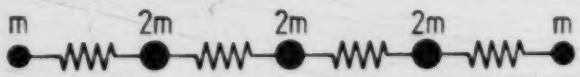

(b) Free-fixed boundary.

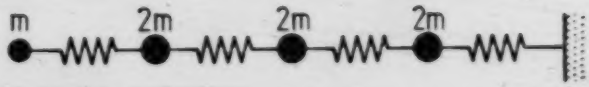

(c) Fixed-fixed boundary.

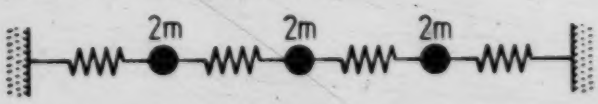

Figure 3.5. Free vibrations of a four span spring-mass system of symmetric elements.

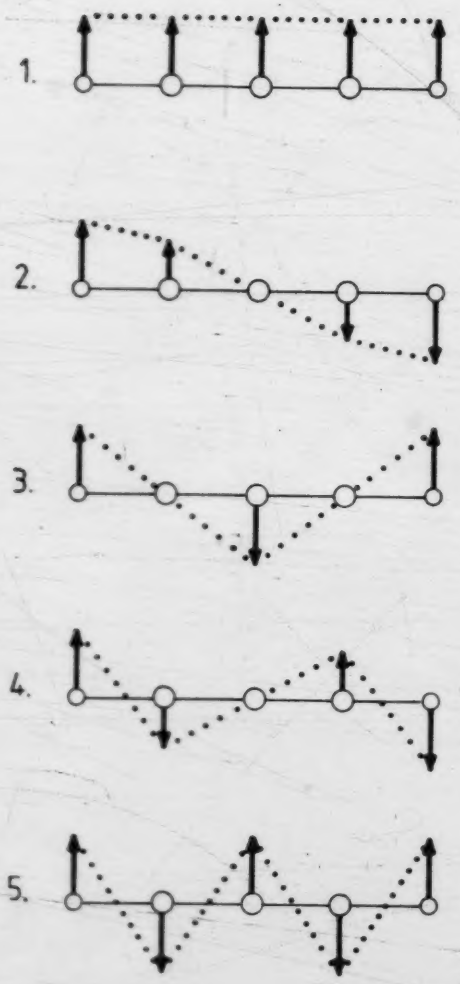

(a) Free-free system.

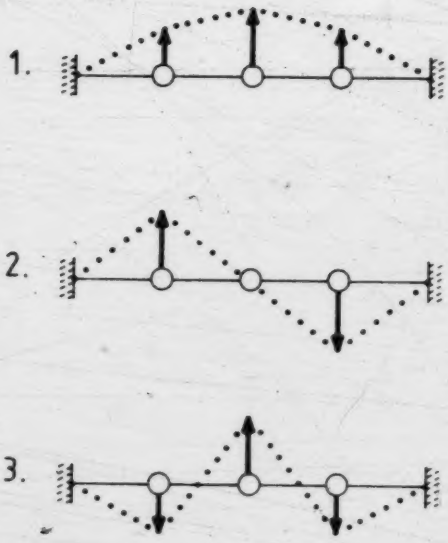

(b) Fixed-fixed system.

Figure 3.6. Mode shapes of the four span spring-mass system.

Table 3.2. Natural frequencies of four span spring-mass systems of unsymmetric elements. ($b=\sqrt{\frac{m}{k}}\omega$)

MODE	FREE-FREE	FREE-FIXED	FIXED-FREE	FIXED-FIXED
1	0.0	0.246	0.315	0.541
2	0.541	0.707	0.882	1.0
3	1.0	1.083	1.274	1.307
4	1.307	1.329		
5	1.414			

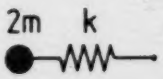

(a) Free-free boundary.

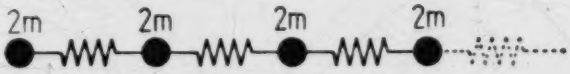

(b) Free-fixed boundary.

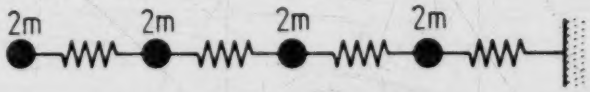

(c) Fixed-free boundary.

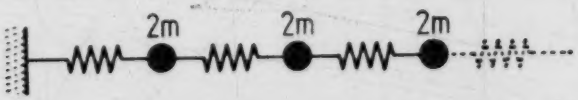

(d) Fixed-fixed boundary.

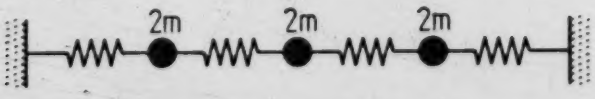

Figure 3.7. Free vibrations of a four span spring-mass system of unsymmetric elements.

Next, consider the spring-mass systems with a unit harmonic force as shown in Figure 3.8. For the first example of the four span free-free system the equation (3.11) can be written as

$$\begin{Bmatrix} X_4 \\ 0 \end{Bmatrix} = [T^4] \begin{Bmatrix} X_0 \\ 1 \end{Bmatrix}. \tag{3.30}$$

From this equation the displacement of the first mass, X_0 can be obtained as

$$\begin{aligned} X_0 &= - t_{22}/t_{21} \\ &= \cosh 4\mu \cdot \sinh\mu / \sinh 4\mu \cdot (2b^2 - b^4). \end{aligned} \tag{3.31}$$

The displacement of the first mass in the next example of free-fixed system in Figure 3.8 can be similarly obtained as

$$\begin{aligned} X_0 &= - t_{12}/t_{11} \\ &= \sinh 4\mu / \sinh\mu \cdot \cosh 4\mu. \end{aligned} \tag{3.32}$$

The displacement of the center mass in the fixed-fixed four span spring-mass system can be also obtained. Since

$$\begin{Bmatrix} 0 \\ F_4 \end{Bmatrix} = [T^4] \begin{Bmatrix} 0 \\ F_0 \end{Bmatrix} + [T^2] \begin{Bmatrix} 0 \\ 1 \end{Bmatrix} \tag{3.33}$$

F_0 can be obtained as

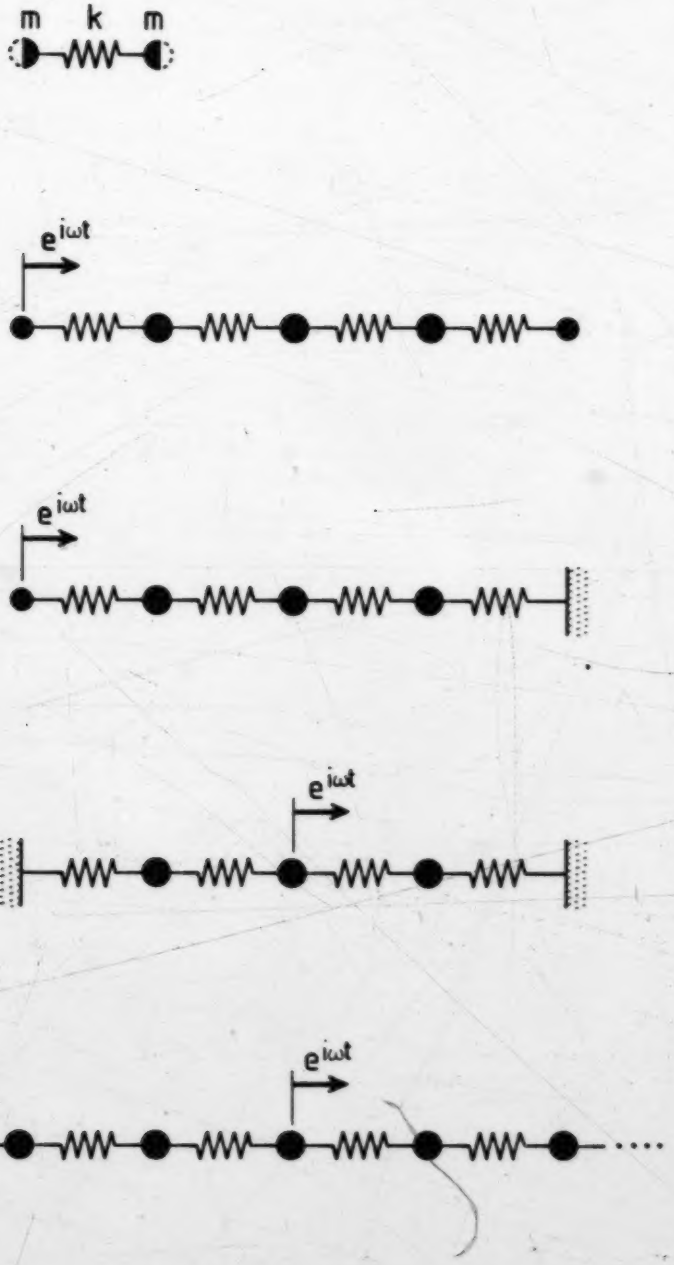

Figure 3.8. Forced responses of symmetric spring-mass systems.

$$F_o = -\sinh 2\mu/\sinh 4\mu. \tag{3.34}$$

The displacement of the center mass, X_2 is then

$$\begin{aligned} X_2 &= t_{12}F_o \\ &= \sinh^2 2\mu/\sinh\mu\cdot\sinh 4\mu \end{aligned} \tag{3.35}$$

where the propagation constant, μ in these equations can be evaluated by the equation (3.25). For the last example of infinite system in Figure 3.8 the response can be obtained by the simpler calculation. Since the eigenvector of the transfer matrix in equation (3.24) is of the form

$$X/F = 1/\pm\sqrt{b^4-2b^2} \tag{3.36}$$

the ratio of displacement to force is the same for all the state vectors as in this equation. The harmonic responses for the four span spring-mass systems in Figure 3.8 obtained as in the equations (3.31)-(3.36) are shown in Figure 3.9(a)-(d).

E. Discussion

The transfer matrix obtained in the previous chapter for a single periodic unit of the periodic structure and the propagation constant obtained from it is used to solve the free or forced vibration problems of the *N* bay structure in this chapter. For this the first step required is to multiply the element transfer matrix in order to obtain the

(a) Free-free four-span system.

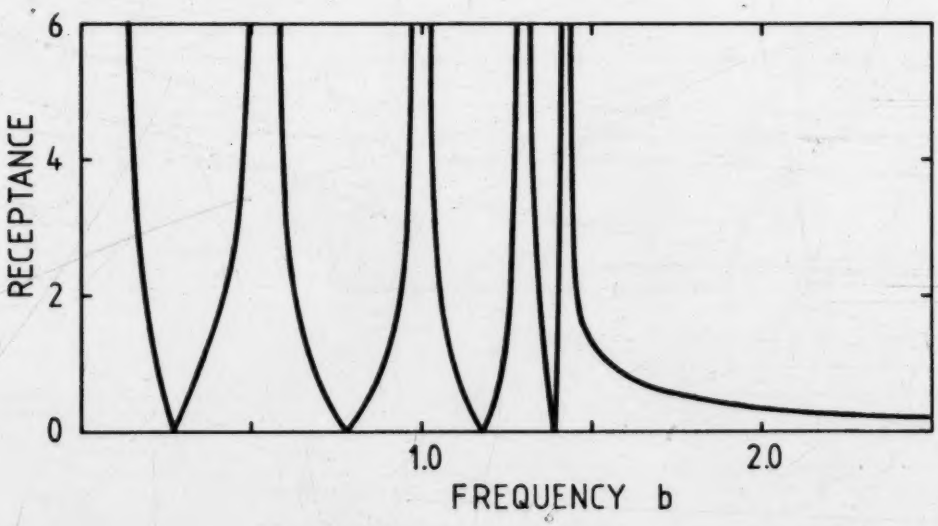

(b) Free-fixed four-span system.

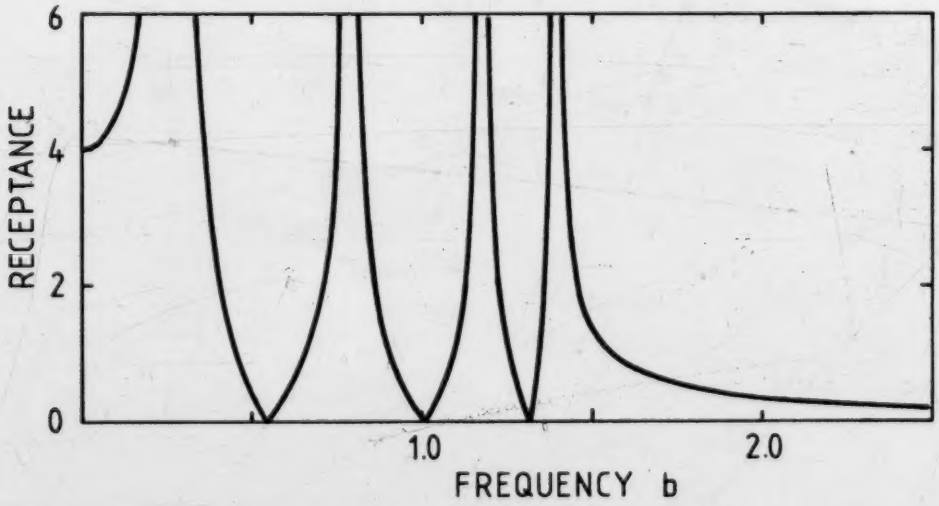

Figure 3.9. Resonance curves of four span spring-mass systems.

(c) Fixed-fixed four-span system.

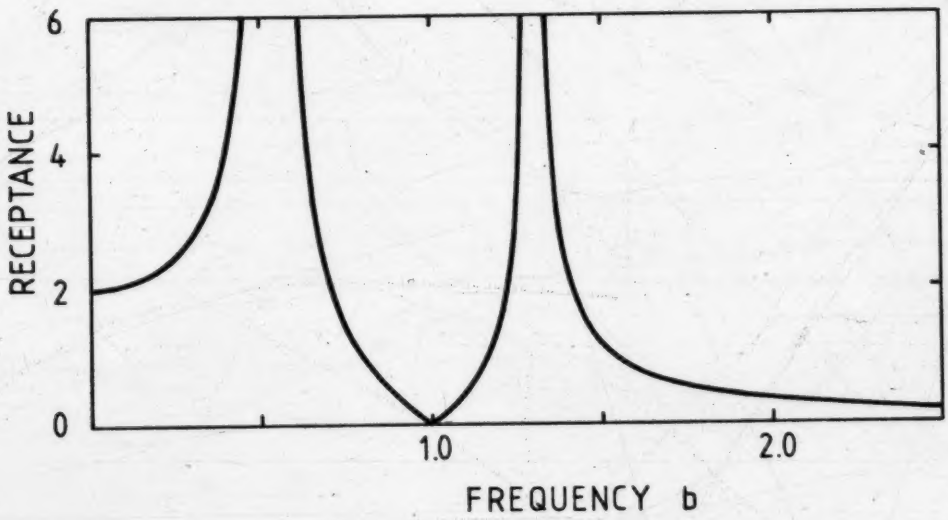

(d) Infinite system.

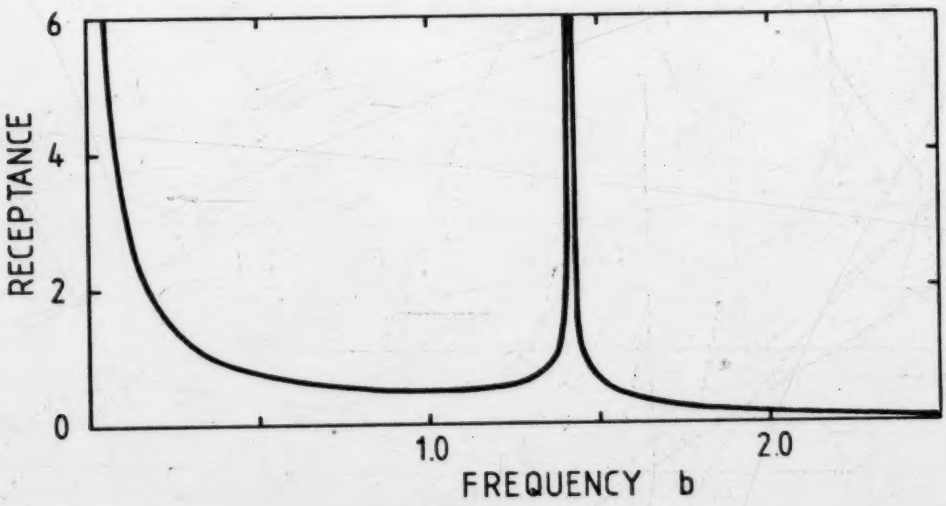

Figure 3.9. continued...

total transfer matrix relating the state vectors at the nodes of several spans apart, eventually from one end to another. It is shown that the use of the Cayley-Hamilton theorem can be made for the mono-coupled system quite effectively.

Many subroutines for the eigenvalues do not require much additional computation to find the eigenvectors. These eigenvectors are simply collected to form the matrix [S] and as in the case of equation (3.10) the inversion of this matrix is not always required. That is, no costly computation with the matrices is involved in such cases. This also increases the accuracy of the numerical results because most round-off errors occur during the matrix multiplication and inversion process. The elaborate numerical scheme of avoiding these calculation errors as in the reference [10] is not necessary in the present study.

The natural frequencies of the periodic structure are found where the determinant of a submatrix vanishes not by the responses becoming infinite as in [10]. Indeed it would be a difficult task to obtain accurate results with calculations involving infinity. The determinantal frequency equations (3.4) and (3.10) can be solved by any numerical techniques available for such equations. However, it was found that the determinant behaves very smoothly around the roots so that even the linear interpolation is quite satisfactory. On the other hand the problem of the steady-state response to harmonic excitation does not

require any iterative numerical scheme, instead the solutions are obtained by a linear equation solver such as Gaussian elimination.

The forced response section is only briefly discussed in this chapter because there are numerous types of problems, many of which are out of the scope of the present study. It is believed that most engineering problems of forced responses can be satisfactorily solved by using the superposition of harmonic responses or by the classical normal mode method using the results obtained by the present method.

In order to treat the infinite structures rigorously the velocities of the waves, group and phase velocities should be considered. However, the infinite structure in this study is not really infinite, instead it approximates a structure with many spans (more than five) with some damping in order to reduce the computational effort still obtaining reasonably good results.

An entire section is devoted to the mono-coupled system because of easy calculation and easy illustration of the method and the behaviour of the solutions. The propagation constant of the mono-coupled system can be either pure imaginary or real with the imaginary part being 0 or $\pm\pi$, in the attenuation zone. For a spring-mass system only the low frequency ($b \leq \sqrt{2}$) signals can propagate along the system so that the system acts like a low pass filter. On the other hand uniform beam on knife-edge supports acts somewhat

like an alternating frequency band pass filter.

For an N bay discrete system with symmetric units, there exist either N or $N-1$ natural frequencies in this propagation zone, with the interval of π/N of the imaginary part of the propagation constant. A system with the mixed boundary has N masses and N natural frequencies all inside the propagation zone. The free-free system has $N+1$ masses and the same number of natural frequencies, of which $N-1$ frequencies lie inside the propagation zone and two are the bounding frequencies. The lower bounding frequency is zero corresponding to rigid body motion leaving N natural frequencies. The fixed-fixed system has $N-1$ masses and $N-1$ natural frequencies all inside the propagation zone.

An N bay continuous system has N natural frequencies in each propagation zone. All the N natural frequencies lie inside the propagation zone in the case of mixed boundary system; while the systems with free-free or fixed-fixed boundaries have $N-1$ natural frequencies inside the propagation zone together with one of the bounding frequencies.

This graphical technique of finding the natural frequencies was first noted by Sen Gupta [20] by considering the flexural waves along the uniform Bernoulli-Euler beam resting on the knife-edge supports, which is an example of the mono-coupled, continuous system as shown in Figure 3.3(b). Figure 3.10 shows the propagation constant for such beams with no rotational springs attached and his method of

determining the natural frequencies of the four span hinged-hinged beams. Unlike the spring-mass system, the attenuation and propagation zones alternate. There is a group of *N* natural frequencies in each propagation zone, and there are infinitely many such groups resulting in infinitely many natural frequencies. This method of finding the natural frequencies of the uniform Bernoulli-Euler beams on knife-edge supports is identical to that employed for the mono-coupled systems in the previous section. In his study, however, the limitations of this graphical technique are not clear. In the present study the mono-coupled system is just a special case where the present method of analysis applies and in the procedure of the analysis the graphical technique appears. It is now clear that this graphical technique can be applied to any mono-coupled system, whether it is a uniform beam (Timoshenko or Bernoulli-Euler beam) on knife-edge supports, spring-mass oscillation system or even some electrical circuits. When the periodic element is not symmetric about its center, however, the natural frequencies of the system with unsymmetric boundaries, i.e., one end free and the other fixed, can not be obtained graphically, instead the equation (3.23) is to be used.

It can be noted that the symmetric and the anti-symmetric modes alternate in the case of symmetric systems in Figure 3.6. At each of the natural frequencies of the free-free system including the first one which represents the rigid body motion, the end masses must

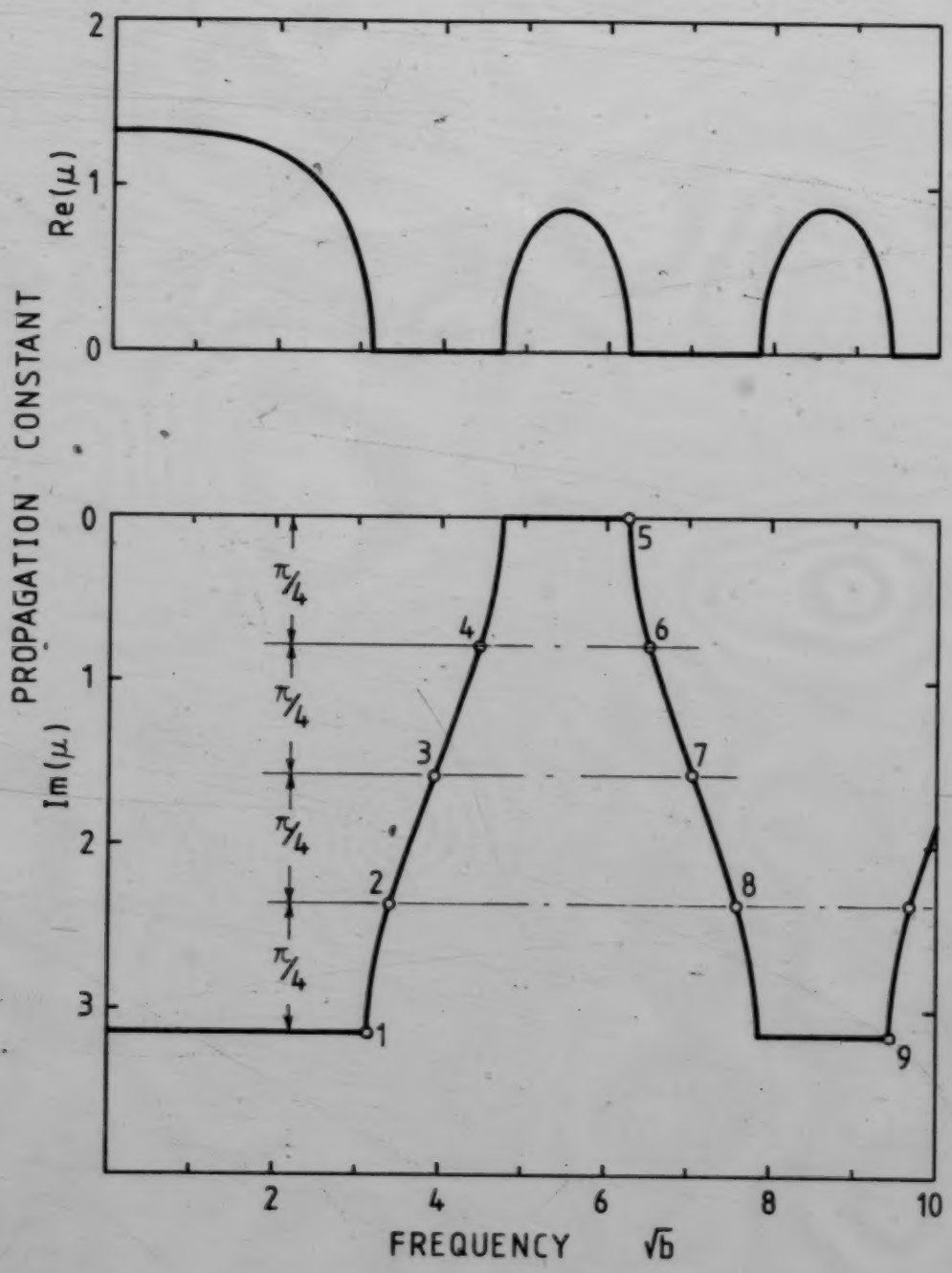

Figure 3.10. Propagation constant for a Bernoulli-Euler beam resting on knife-edge supports.

oscillate so that if the excitation is introduced at the end the resonance must occur. However, if the center mass of the fixed-fixed system is excited, the resonance can occur only at the first and third natural frequencies corresponding to the symmetric modes. This may be observed in Figures 3.9 (a) and (c).

Harmonically excited steady-state responses are obtained in the form of receptance (ratio of displacement to force [2]) for the four span spring-mass systems with four different boundary conditions and the results are shown in the resonance curves, Figure 3.9(a)-(d). Unlike the single mass system the response can become zero, that is, a force can be exerted into the system with no motion at the point of excitation; the system is acting like a vibration absorber. Since the curves show only the absolute value of the displacement to force ratio the phase difference of input and output is not seen from these figures instead it can be noted from the equations (3.31)-(3.36). The receptance in equation (3.36) is pure imaginary when $b \leq \sqrt{2}$ so that there exists 0.5π phase difference in the infinite system. The free-free system is capable of rigid body motion so that the receptance is infinite at zero frequency (static load), but as soon as the exciting force becomes harmonic with low frequency the displacement becomes harmonic with π out of phase of the force.

IV. NUMERICAL EXAMPLE - UNIFORM TIMOSHENKO BEAM

A. Introduction

All the formulation in the previous chapter is not restricted to simple types of uniform beams. However, the numerical example taken in this chapter is a uniform Timoshenko beam in which the effect of rotary inertia and shear deformation is fully taken into account.

In this chapter the impedance matrix for a beam element is first obtained. This impedance matrix can be obtained by the Finite Element formulation using Huang's normal modes as the interpolation functions. However, the same impedance matrix is more readily available by the beam flexural theory and the unknown coefficient method. The analytical transfer matrix for a Timoshenko beam is then derived from this impedance matrix and expressed in terms of Huang's normal mode solutions and his notations.

Natural frequencies of the uniform Timoshenko beam on the knife-edge supports are found by a graphically illustrated technique as explained in section III.D, although the actual calculation is done by a digital computer. The natural frequencies of beams on spring supports are found by solving the determinantal frequency equations. The configuration of the intermediate supports is changed by varying the translational spring constant, k_t and the rotational spring, k_r. For example, the beam resting on the knife-edge supports can be represented either by a

beam with k_t becoming infinite, or by eliminating the deflection and the shear force at the nodes since only the bending slope and the bending moment can be transmitted through the knife-edge supports.

The rotational spring in Figure 4.1 is assumed to exert a resisting moment proportional to the bending slope instead of the total slope. Consequently, the boundary condition at the clamped end of the Timoshenko beam is implemented by equating the bending slope to zero. This assumption makes the calculation simpler, although it would make no difference in the case of the Bernoulli-Euler beam where the bending slope and the total slope are the same.

The results of the harmonic response problems are presented in the form of resonance curves. Infinite boundary conditions are also considered together with the ordinary boundary conditions such as hinged or clamped.

In order to show the effect of rotary inertia and shear deformation, the results are obtained for the three slenderness ratios; r=0, 0.04 and 0.08. When this slenderness ratio is set to zero the cross-sectional dimension is in fact neglected and hence the results become those for the Bernoulli-Euler beam.

Little work has been done for the Timoshenko beam on multiple supports, mainly due to the complexity of the problem. The analytical solution by the present method therefore can not be confirmed by other published results. However, the results for some extreme cases of zero

slenderness ratio or the single span beam may be compared with those in [2], [5], [9] and [10]. For this purpose the spring constants and other parameters are chosen as those found in these references.

B. Analytical Formulation of Transfer Matrix

Timoshenko beam differential equation

Consider a continuous beam shown in Figure 4.1(b). The elastic constraints provided at each support are characterized by a translational spring, k_t and a rotational spring, k_r. All the interior supports are assumed to be identical maintaining the periodicity of the structure.

(a) Knife-edge supports.

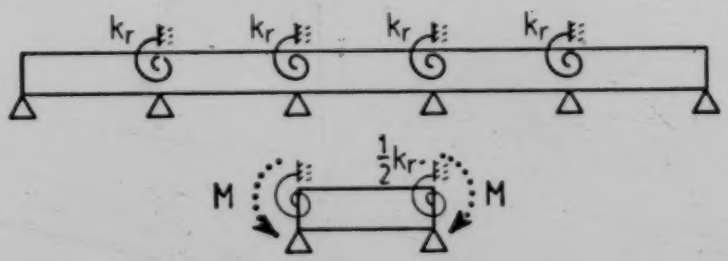

(b) Spring supports.

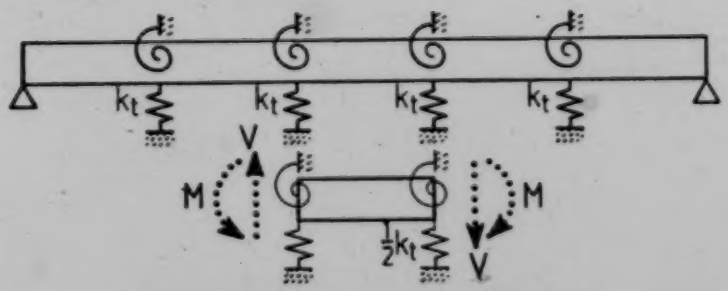

Figure 4.1. Uniform beams resting on equi-spaced supports.

The coupled equations for the total deflection, y and ψ, the slope due to bending within a span are due to Timoshenko[21]

$$EI\frac{\partial^2\psi}{\partial x^2}+k'GA\left(\frac{\partial y}{\partial x}-\psi\right)-\rho I\frac{\partial^2\psi}{\partial t^2}=0 \qquad (4.1)$$

$$\rho A\frac{\partial^2 y}{\partial t^2}-k'GA\left(\frac{\partial^2 y}{\partial x^2}-\frac{\partial\psi}{\partial x}\right)=0 \qquad (4.2)$$

in which

A = cross-sectional area

E = Young's modulus of elasticity

G = shear modulus

I = area moment of inertia of cross-section

k' = shape factor for cross-section

ρ = mass density of material.

Setting

$$y = lY\exp(i\omega t) \qquad (4.3)$$

$$\psi = \Psi\exp(i\omega t) \qquad (4.4)$$

$$\xi = x/l \qquad (4.5)$$

where

Y = normal function of y

Ψ = normal function of ψ

ξ = nondimensional local coordinate

ω = angular frequency

l = length of a beam segment,

yields

$$s^2\Psi''-(1-b^2r^2s^2)\Psi+Y'=0 \tag{4.6}$$

$$Y''+b^2s^2Y-\Psi'=0. \tag{4.7}$$

Eliminating Ψ or Y from equations (4.6) and (4.7), the following differential equations are obtained

$$Y^{IV}+b^2(r^2+s^2)Y''-b^2(1-b^2r^2s^2)Y=0 \tag{4.8}$$

$$\Psi^{IV}+b^2(r^2+s^2)\Psi''-b^2(1-b^2r^2s^2)\Psi=0. \tag{4.9}$$

In equations (4.6)-(4.9) the nondimensional parameters b, s, r are defined as

$$b^2=\frac{\rho A}{EI}l^4\omega^2 \tag{4.10}$$

$$r^2=\frac{I}{Al^2} \tag{4.11}$$

$$s^2=\frac{E}{k'G}\frac{I}{Al^2} \tag{4.12}$$

and the prime indicates the differentiation with respect to the nondimensional local coordinate ξ.

Following Huang's procedure further, the normal mode solutions to equations (4.8)-(4.9) are found as

$$Y=C_1\cosh p\xi+C_2\sinh p\xi+C_3\cos q\xi+C_4\sin q\xi \tag{4.13}$$

$$\Psi = D_1 \cosh p\xi + D_2 \sinh p\xi + D_3 \cos q\xi + D_4 \sin q\xi \qquad (4.14)$$

where

$$\frac{p}{q} = \frac{b}{\sqrt{2}} \sqrt{\mp (r^2+s^2) + \sqrt{(r^2-s^2)^2 + \frac{4}{b^2}}} \quad . \qquad (4.15)$$

The argument of the hyperbolic normal functions, p in equation (4.15) can become imaginary number when the term in the square root bracket becomes negative. This extension is applied to all the consequent equations involving with p. The coefficients C_1, C_2,.. and D_1, D_2,.. are related by equations (4.6) or (4.7) as

$$\begin{aligned} D_1 &= \alpha C_2 \\ D_2 &= \alpha C_1 \\ D_3 &= \beta C_4 \\ D_4 &= -\beta C_3 \end{aligned} \qquad (4.16)$$

where α and β are the nondimensional constants defined by $\alpha = p + b^2 s^2/p$, $\beta = q - b^2 s^2/q$.

From the beam flexure theory the nondimensional shear force V and the bending moment M can be expressed as [21]

$$V = - \{k'GA(\partial y/\partial x - \psi)\} l^2/EI \qquad (4.17)$$

$$M = - l \partial \psi/\partial x. \qquad (4.18)$$

Substituting equations (4.1)-(4.5) into equations

(4.17)-(4.18) the generalized forces are obtained as

$$\begin{aligned} V &= (b^2 r^2 \Psi + \Psi'')\exp(i\omega t) \\ M &= -\Psi' \exp(i\omega t). \end{aligned} \tag{4.19}$$

Having the expressions for the generalized displacements, equations (4.13)-(4.14), and forces, equations (4.19)-(4.20), it is possible to define a state vector as

$$\{v\} = \begin{Bmatrix} Y \\ \Psi \\ V \\ M \end{Bmatrix} = \begin{Bmatrix} Y \\ \Psi \\ b^2 r^2 \Psi + \Psi'' \\ -\Psi' \end{Bmatrix}. \tag{4.20}$$

Here the common factor $\exp(i\omega t)$ was omitted, and all the elements of the vector $\{v\}$ are nondimensional quantities. Using the normal mode solution, equation (4.13) and (4.14), the generalized displacements and forces at the left and right ends of the beam segment are expressed in terms of unknown constants $\{C\}$.

$$\begin{Bmatrix} Y(\xi=0) \\ \Psi(\xi=0) \\ Y(\xi=1) \\ \Psi(\xi=1) \end{Bmatrix} = \begin{bmatrix} 1 & 0 & 1 & 0 \\ 0 & \alpha & 0 & \beta \\ Ch & Sh & C & S \\ \alpha Sh & \alpha Ch & -\beta S & \beta C \end{bmatrix} \begin{Bmatrix} C_1 \\ C_2 \\ C_3 \\ C_4 \end{Bmatrix}, \tag{4.21}$$

$$\begin{Bmatrix} V(\xi=0) \\ M(\xi=0) \\ V(\xi=1) \\ M(\xi=1) \end{Bmatrix} = \begin{bmatrix} 0 & q\alpha\beta & 0 & -p\alpha\beta \\ -p\alpha & 0 & q\beta & 0 \\ q\alpha\beta Sh & q\alpha\beta Ch & p\alpha\beta S & -p\alpha\beta C \\ p\alpha Ch & p\alpha Sh & -q\beta C & -q\beta S \end{bmatrix} \begin{Bmatrix} C_1 \\ C_2 \\ C_3 \\ C_4 \end{Bmatrix} \tag{4.22}$$

where Ch, Sh, C and S denote the four normal functions, coshp, sinhp, cosq and sinq, respectively, and the relationship

$$p^2+b^2r^2 = q\beta$$
$$q^2-b^2r^2 = p\alpha \qquad (4.23)$$

was used to simplify the expression.

Impedance matrix

The impedance matrix which relates the generalized displacements and forces is then obtained by substituting for the constants {C} in equation (4.22) with the displacements obtained from equation (4.21) as

$$[Z] = \frac{p^2+q^2}{(\alpha^2-\beta^2)ShS+2\alpha\beta(1-ChC)} \begin{bmatrix} z_{11} & z_{12} & z_{13} & z_{14} \\ z_{21} & z_{22} & z_{23} & z_{24} \\ z_{31} & z_{32} & z_{33} & z_{34} \\ z_{41} & z_{42} & z_{43} & z_{44} \end{bmatrix} \qquad (4.24)$$

where z_{ij} denote the components of [Z]:

$$z_{11} = \alpha\beta(\alpha ShC+\beta ChS)$$
$$z_{12} = \alpha\beta\{ShS+(q\beta-p\alpha)(1-ChC)\}/(p^2+q^2)$$
$$z_{13} = -\alpha\beta(\alpha Sh+\beta S)$$
$$z_{14} = \alpha\beta(Ch-C)$$
$$z_{22} = \alpha ChS-\beta ShC \qquad (4.25)$$
$$z_{23} = -\alpha\beta(Ch-C)$$
$$z_{24} = \beta Sh-\alpha S$$
$$z_{33} = z_{11}$$

$$z_{34} = -z_{12}$$

$$z_{44} = z_{22}.$$

The same impedance matrix would be obtained by the standard finite element formulation procedure, with the interpolation functions being taken as the four exponential functions or two trigonometric and two hyperbolic functions. However, the method described in this section is much simpler in the case of an analytical impedance matrix.

The forces due to springs (translational or rotational) are not included in equation (4.25), however the effect of springs at each end of the subsystem can be included easily by adding to equation (4.25) the matrix

$$[Z] = \begin{bmatrix} k_1 & & & \\ & k_2 & & \\ & & k_1 & \\ & & & k_2 \end{bmatrix} \tag{4.26}$$

where k_1, k_2 are nondimensional spring constants defined as

$$\begin{aligned} k_1 &= k_t l^3/2EI, \\ k_2 &= k_r l/2EI. \end{aligned} \tag{4.27}$$

Transfer matrix and its inverse

Once the impedance matrix is obtained, the expression for the transfer matrix can be easily derived by the simple algebraic procedure described in the previous chapter. The

final expression of the transfer matrix for the Timoshenko beam element shown in Figure 4.1(b) is obtained as

$$[T] = \frac{1}{p^2+q^2} \cdot \begin{bmatrix} t_{11} & t_{12} & t_{13} & t_{14} \\ t_{21} & t_{22} & t_{23} & t_{24} \\ t_{31} & t_{32} & t_{33} & t_{34} \\ t_{41} & t_{42} & t_{43} & t_{44} \end{bmatrix}$$

where

$$\begin{aligned}
t_{11} &= q\beta Ch+p\alpha C - k_1(Sh/\alpha-S/\beta \\
t_{12} &= pSh+qS + k_2(Ch-C) \\
t_{13} &= (\beta Sh-\alpha S)/\alpha\beta \\
t_{14} &= Ch-C \\
t_{21} &= \alpha\beta(qSh-pS) - k_1(Ch-C) \\
t_{22} &= p\alpha Ch+q\beta C + k_2(\alpha Sh+\beta S) \\
t_{23} &= Ch-C \\
t_{24} &= \alpha Sh+\beta S \\
t_{31} &= \alpha\beta(q^2\beta Sh+p^2\alpha S) - 2k_1(q\beta Ch+p\alpha C)+k_1^2(Sh/\alpha-S/\beta) \\
t_{32} &= b^2(Ch-C) - k_1(pSh+qS)+k_2\alpha\beta(qSh-pS)-k_1k_2(Ch-C) \\
t_{33} &= q\beta Ch+p\alpha C - k_1(Sh/\alpha-S/\beta) \\
t_{34} &= \alpha\beta(qSh-pS) + k_1(Ch-C) \\
t_{41} &= b^2(Ch-C) + k_1(pSh+qS)-k_2\alpha\beta(qSh-pS)+k_1k_2(Ch-C) \\
t_{42} &= p^2\alpha Sh-q^2\beta S - 2k_2(p\alpha Ch+q\beta C)-k_2^2(\alpha Sh+\beta S) \\
t_{43} &= pSh+qS - k_2(Ch-C) \\
t_{44} &= p\alpha Ch+q\beta C + k_2(\alpha Sh+\beta S).
\end{aligned} \tag{4.28}$$

This transfer matrix can also be obtained directly from the normal mode functions and beam flexure theory without formulating the impedance matrix as shown in Appendix B.

C. Special Cases

As mentioned previously, the general transfer matrix for the Timoshenko beam, equation (4.28), can be reduced to that for Bernoulli-Euler beam by simply putting the slenderness ratio to zero, i.e., $r^2=s^2=0$, so that

$$p=q=\alpha=\beta=\sqrt{b}. \tag{4.29}$$

The transfer matrix for the Bernoulli-Euler beam on spring supports then becomes a 4x4 matrix:

$$[T] = \frac{1}{2} \cdot \begin{bmatrix} t_{11} & t_{12} & t_{13} & t_{14} \\ t_{21} & t_{22} & t_{23} & t_{24} \\ t_{31} & t_{32} & t_{33} & t_{34} \\ t_{41} & t_{42} & t_{43} & t_{44} \end{bmatrix}$$

where

$$\begin{aligned}
t_{11} &= p^3(Ch+C) - k_1(Sh-S) \\
t_{12} &= p^2(Sh+S) + k^2p(Ch-C) \\
t_{13} &= Sh-S \\
t_{14} &= p(Ch-C) \\
t_{21} &= p^2(Sh-S) - k_1p(Ch-C) \\
t_{22} &= p^3(Ch+C) \\
t_{23} &= p(Ch-C) \\
t_{24} &= p^2(Sh+S) \\
t_{31} &= p^4(Sh+S) - 2k_1p^3(Ch+C)+k_1^2(Sh-S) \\
t_{32} &= p^5(Ch-C) - k_1p^2(Sh+S)+k_2p^4(Sh-S)-k_1k_2p(Ch-C) \\
t_{33} &= p^3(Ch+C) - k_1(Sh-S) \\
t_{34} &= p^4(Sh-S) - k_1p(Ch-C) \\
t_{41} &= p^5(Ch-C) - k_1p^2(Sh+S)+k_2p^4(Sh-S)-k_1k_2p(Ch-C)
\end{aligned} \tag{4.30}$$

$$t_{42} = p^4(Sh-S) + 2k_2p^3(Ch+C)+k_2^2p^2(Sh+S)$$

$$t_{43} = p^2(Sh+S) + k_2p(Ch-C)$$

$$t_{44} = p^3(Ch+C) + k_2p^2(Sh+S).$$

A special case of this development is the beam on knife-edge supports, which was considered by Miles[16] and Ayre and Jacobsen[1]. The transfer matrix in this case can be obtained by setting the total deflection y to zero on the supports. The transfer matrix obtained from equations (4.28) and (4.30) by this operation as shown in Appendix C is for the Timoshenko beam

$$[T] = \frac{1}{\beta Sh-\alpha S}\cdot \begin{bmatrix} \beta ShC-\alpha ChS-k_2\Delta & \Delta \\ (p^2+q^2)ShS-2k_2(\beta ShC-\alpha ChS)+k_2^2\Delta & \beta ShC-\alpha ChS-k_2\Delta \end{bmatrix} \tag{4.31}$$

where $\Delta=\{(\alpha^2-\beta^2)ShS+2\alpha\beta(1-ChC)\}/(p^2+q^2)$.

For the Bernoulli-Euler beam

$$[T] = \frac{1}{Sh-S}\cdot \begin{bmatrix} ShC-ChS-k_2(1-ChC)/p & (1-ChC)/p \\ 2pShS-2k_2(ShC-ChS)+k_2^2(1-ChC)/p & ShC-ChS-k_2(1-ChC)/p \end{bmatrix}. \tag{4.32}$$

Using the equations (2.25)-(2.26) the total transfer matrices for the N-span beams can be obtained in terms of the propagation constant and the normal mode functions either for the Timoshenko or the Bernoulli-Euler beams.

D. Natural Frequencies

Timoshenko beams on knife-edge supports

Figure 4.2 shows a uniform beam resting on the knife-edge supports with a rotational spring provided at each support. The propagation constants are obtained for a beam element with three different k_2 values; k_2=0, 1 and 100, and shown in Figures 4.3-5. From these propagation constant curves and by the graphical techniques as explained in the section III.D, the natural frequencies are obtained for two different boundary conditions; hinged and clamped. The first four natural frequencies for the four-span beams are listed in Table 4.1. The corresponding mode shapes are shown for the hinged beam case in Figure 4.6. Shown is the total deflection as well as that due to bending alone.

(a) Hinged-hinged boundary.

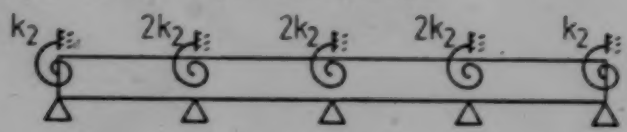

(b) Clamped-clamped boundary.

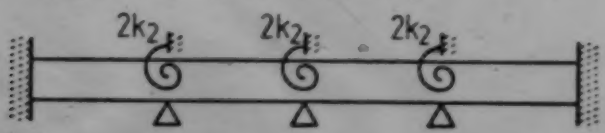

Figure 4.2. Free vibrations of the uniform beams on knife-edge supports.

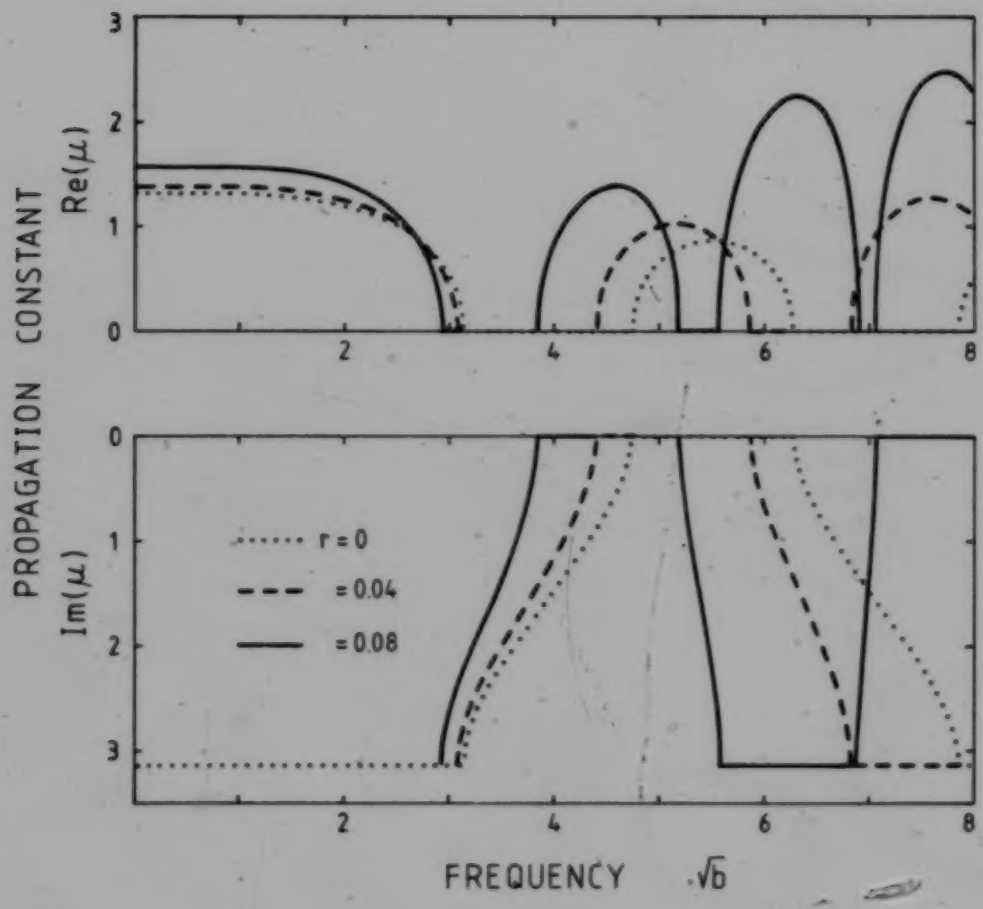

Figure 4.3. Propagation constant with k_z=0.

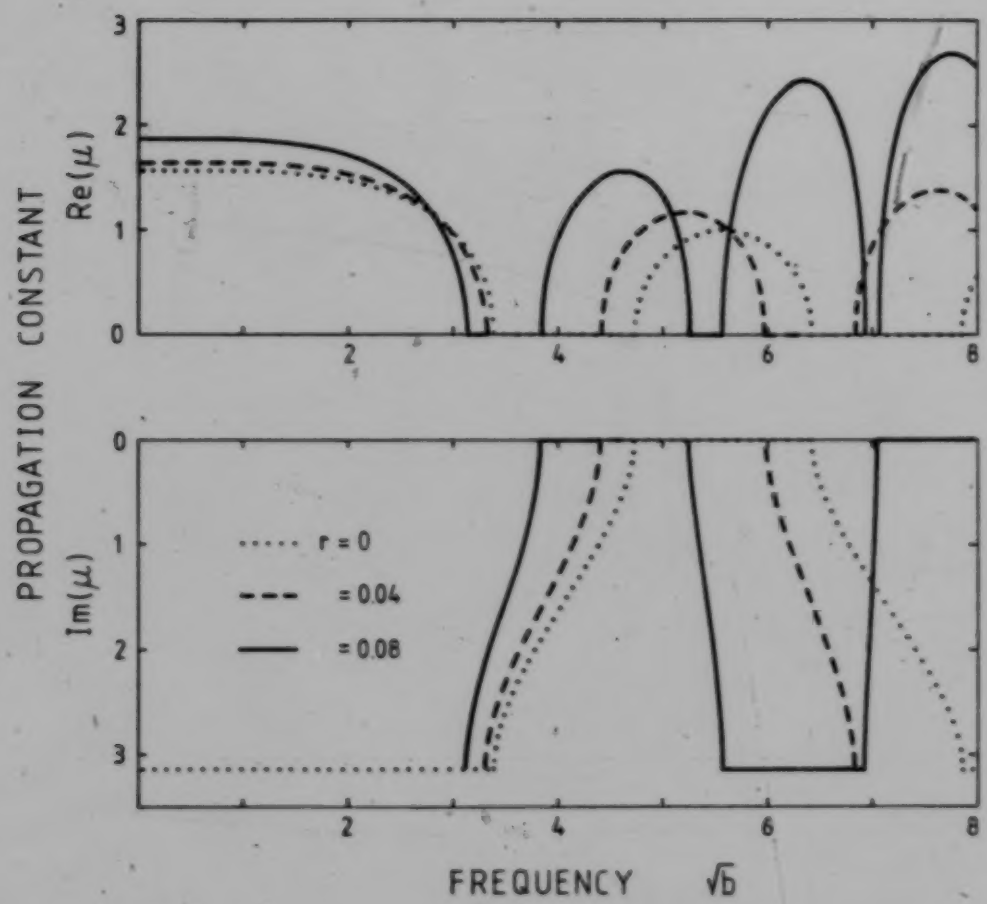

Figure 4.4. Propagation constant with $k_2=1$.

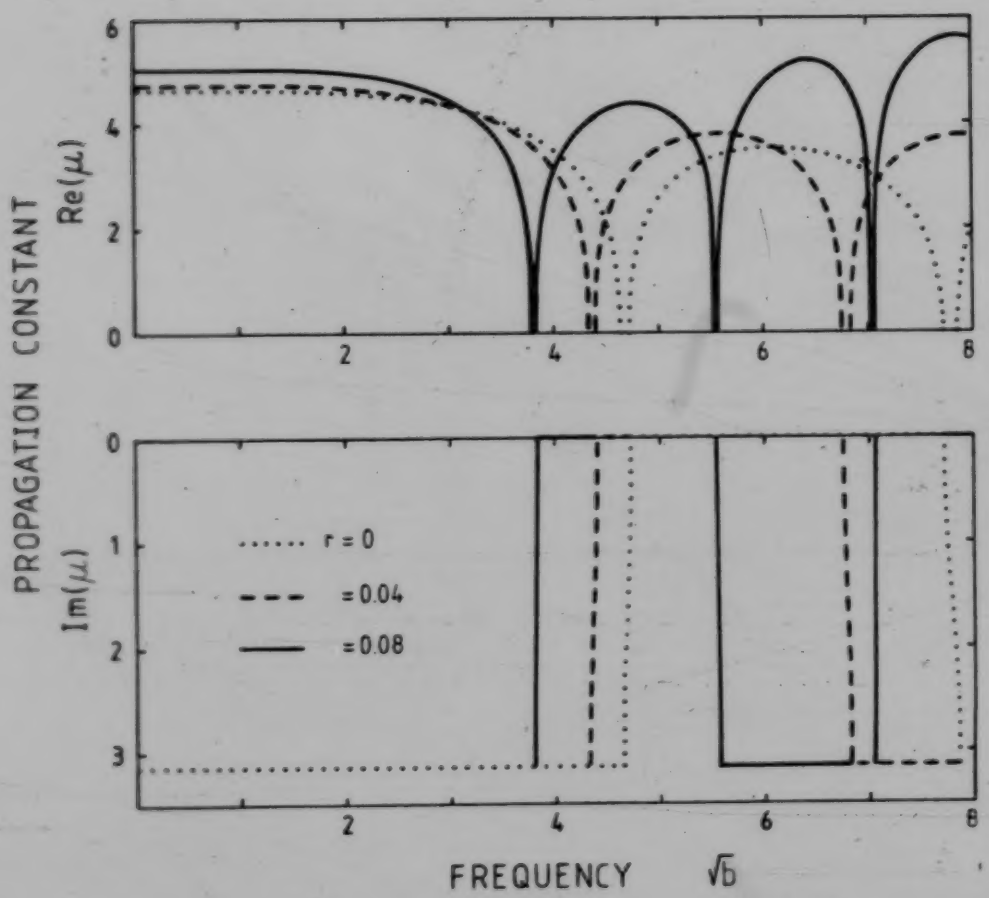

Figure 4.5. Propagation constant with k_2=100.

Table 4.1. Natural frequencies of a four span beam on knife-edge supports, $\sqrt{b}=\{\rho A l^4\omega^2/EI\}^{1/4}$.

(a) $k_2 = 0$.

	r = 0		0.04		0.08	
MODE	HINGE	CLAMP	HINGE	CLAMP	HINGE	CLAMP
1	3.142	3.393	3.083	3.301	2.940	3.090
2	3.393	3.926	3.301	3.759	3.090	3.412
3	3.926	4.464	3.759	4.199	3.412	3.709
4	4.464	4.730	4.199	4.402	3.709	3.833

(b) $k_2 = 1$.

	r = 0		0.04		0.08	
MODE	HINGE	CLAMP	HINGE	CLAMP	HINGE	CLAMP
1	3.397	3.596	3.316	3.486	3.126	3.241
2	3.596	4.042	3.486	3.860	3.241	3.492
3	4.042	4.505	3.860	4.233	3.492	3.733
4	4.505	4.730	4.233	4.402	3.733	3.833

(c) $k_2 = 100$.

	r = 0		0.04		0.08	
MODE	HINGE	CLAMP	HINGE	CLAMP	HINGE	CLAMP
1	4.642	4.654	4.337	4.347	3.799	3.804
2	4.654	4.685	4.347	4.370	3.804	3.816
3	4.685	4.717	4.370	4.392	3.816	3.828
4	4.717	4.730	4.392	4.402	3.828	3.833

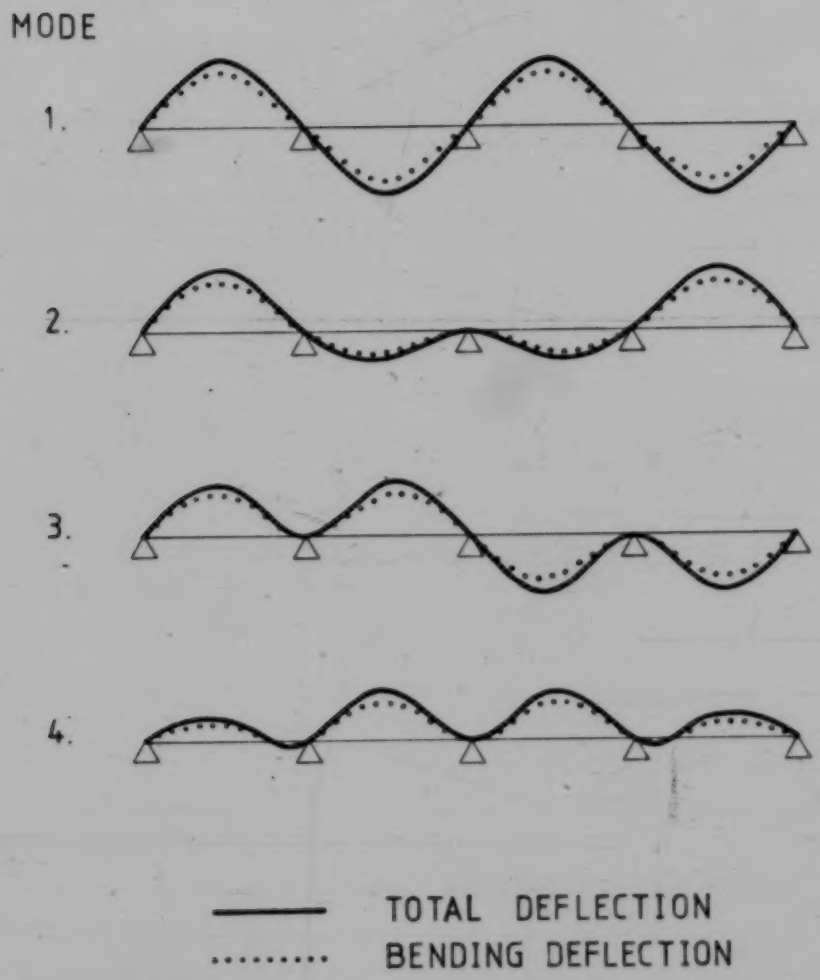

Figure 4.6. Normal modes of the four span Timoshenko beam on knife-edge supports.

Timoshenko beams on elastic springs

Figure 4.7 shows the beam supported on elastic translational and rotational springs. Natural frequencies are found for three different k_1 values; k_1=0, 0.5 and 50, and for two different boundary conditions, hinged and clamped. The rotational spring, k_2 is assumed zero for all the results presented, although it can be easily included. Again the first four natural frequencies given in Table 4.2 are for the four-span beams. In Figure 4.8 the corresponding mode shapes are shown for the hinged beam case. Shown is the total deflection as well as the portion of the deflection due to bending alone.

(a) Hinged-hinged boundary.

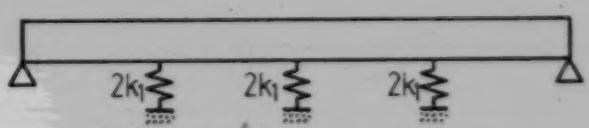

(b) Clamped-clamped boundary.

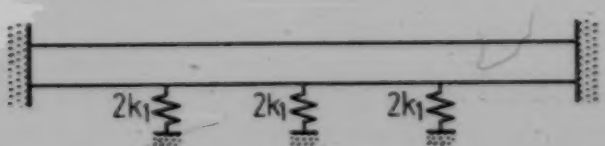

Figure 4.7. Free vibration of the beams on spring supports.

Table 4.2. Natural frequencies of a four span beam on spring supports, $\sqrt{b}=\{\rho A\}^{\frac{1}{4}}\omega^{\frac{1}{2}}/EI\}^{\frac{1}{4}}$.

(a) $k_1 = 0$.

	r = 0		0.04		0.08	
MODE	HINGE	CLAMP	HINGE	CLAMP	HINGE	CLAMP
1	0.785	1.183	0.784	1.176	0.782	1.159
2	1.571	1.963	1.563	1.940	1.542	1.879
3	2.356	2.749	2.331	2.694	2.264	2.558
4	3.142	3.534	3.085	3.446	2.941	3.185

(b) $k_1 = 0.5$.

	r = 0		0.04		0.08	
MODE	HINGE	CLAMP	HINGE	CLAMP	HINGE	CLAMP
1	1.084	1.311	1.083	1.307	1.081	1.294
2	1.631	1.996	1.623	1.974	1.605	1.917
3	2.373	2.766	2.349	2.711	2.284	2.577
4	3.141	3.518	3.082	3.438	2.941	3.185

(c) $k_1 = 50$.

	r = 0		0.04		0.08	
MODE	HINGE	CLAMP	HINGE	CLAMP	HINGE	CLAMP
1	3.028	3.045	2.985	3.005	2.872	2.898
2	3.042	3.065	3.003	3.019	2.897	2.898
3	3.075	3.608	3.025	3.507	2.898	3.288
4	3.142	3.689	3.083	3.562	2.940	3.314

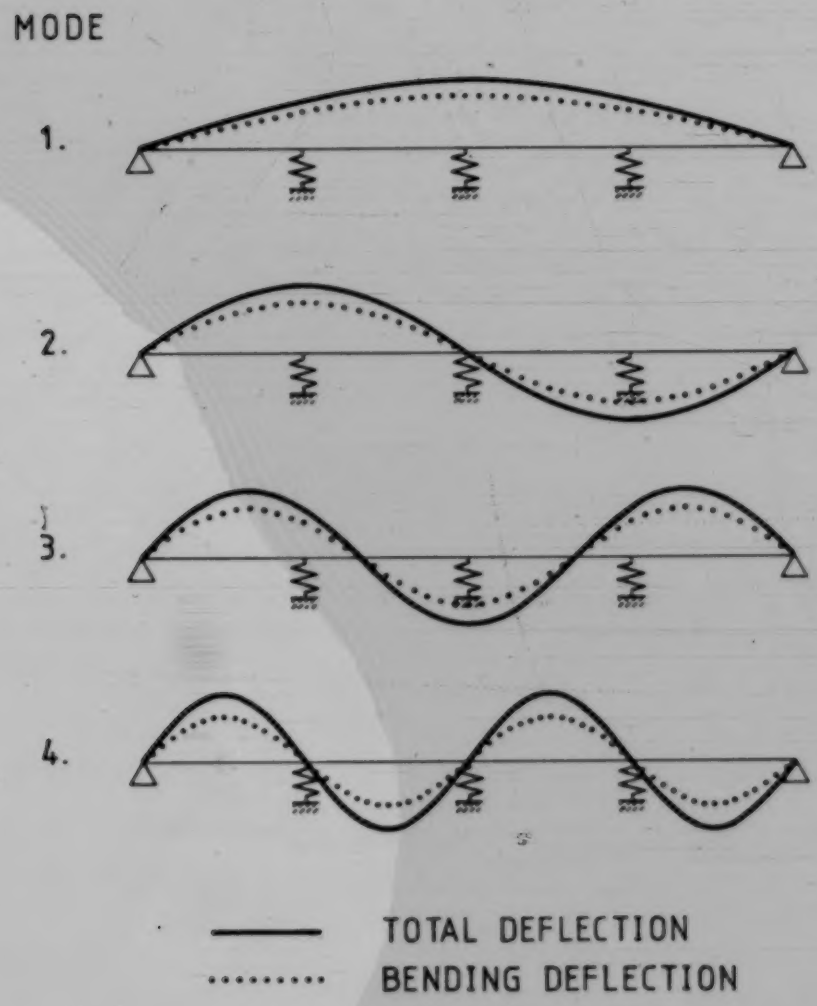

Figure 4.8. Normal modes of the four span Timoshenko beam on spring supports.

E. Steady-state Harmonic Responses

Timoshenko beams on knife-edge supports

A four-span beam with both ends hinged and the beam with infinitely many spans are shown in Figure 4.9. The bending moment is introduced at the center node and the bending slope at the same point is found. The results are then shown by the resonance curves - Figures 4.10 and 4.11.

(a) Four-span hinged-hinged beam.

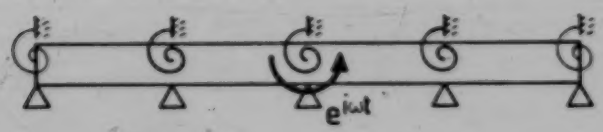

(b) Infinite-infinite beam.

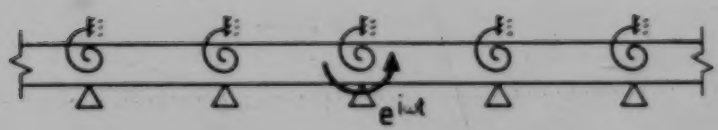

Figure 4.9. Forced vibration of the uniform beams on knife-edge supports.

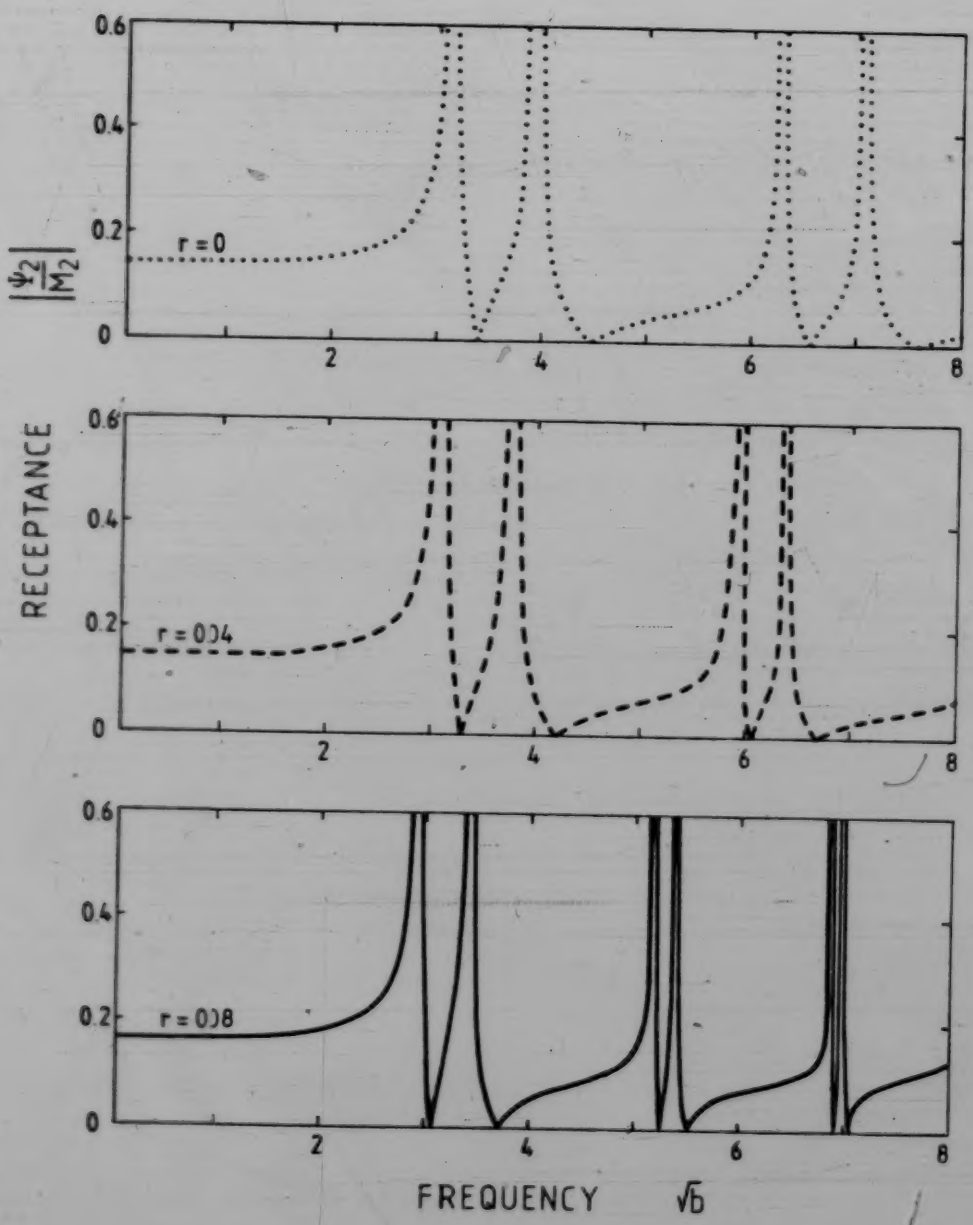

Figure 4.10. Resonance curves of four-span hinged beams.
(a) k_2 =).

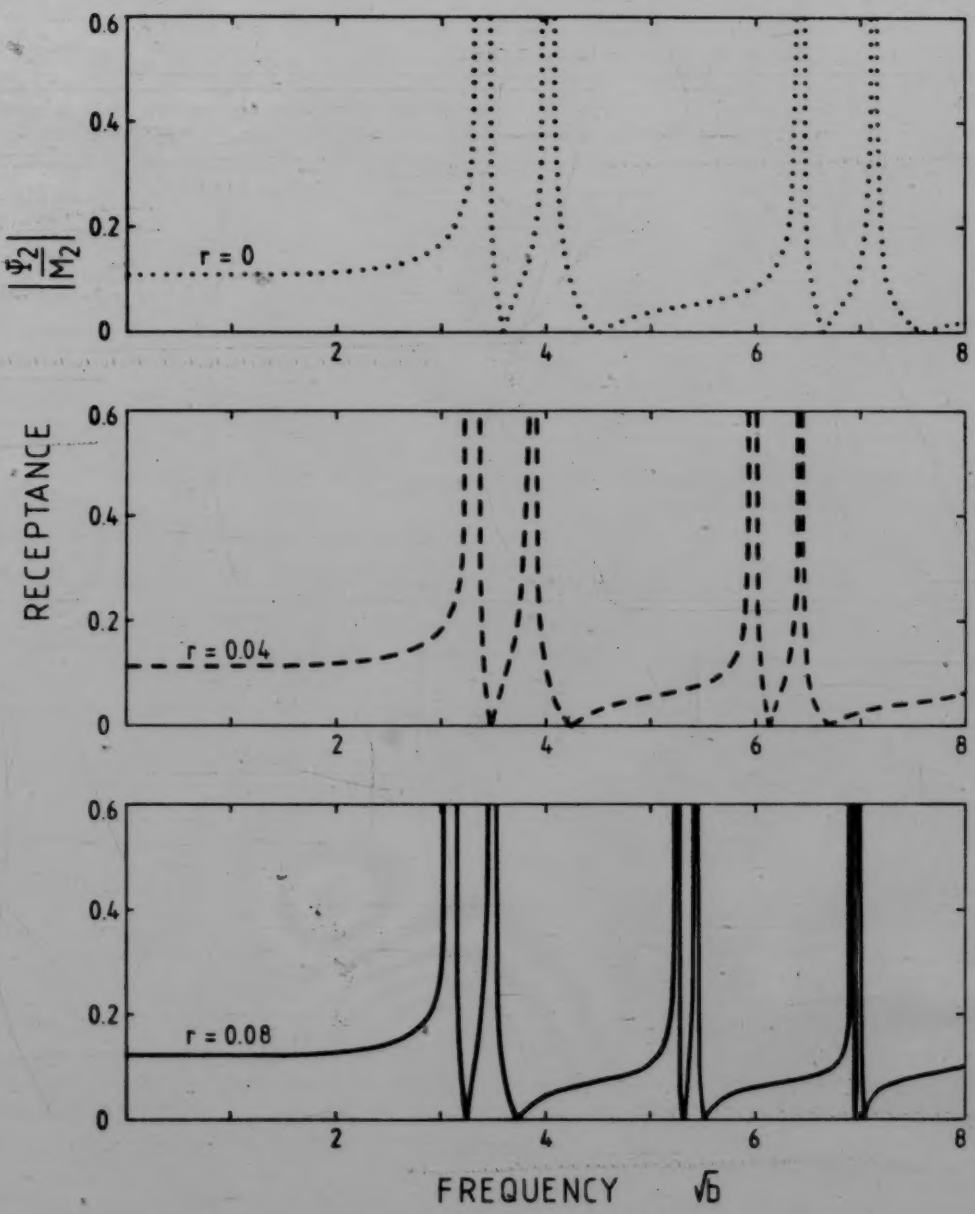

Figure 4.10. continued...

(b) $k_2 = 1.$

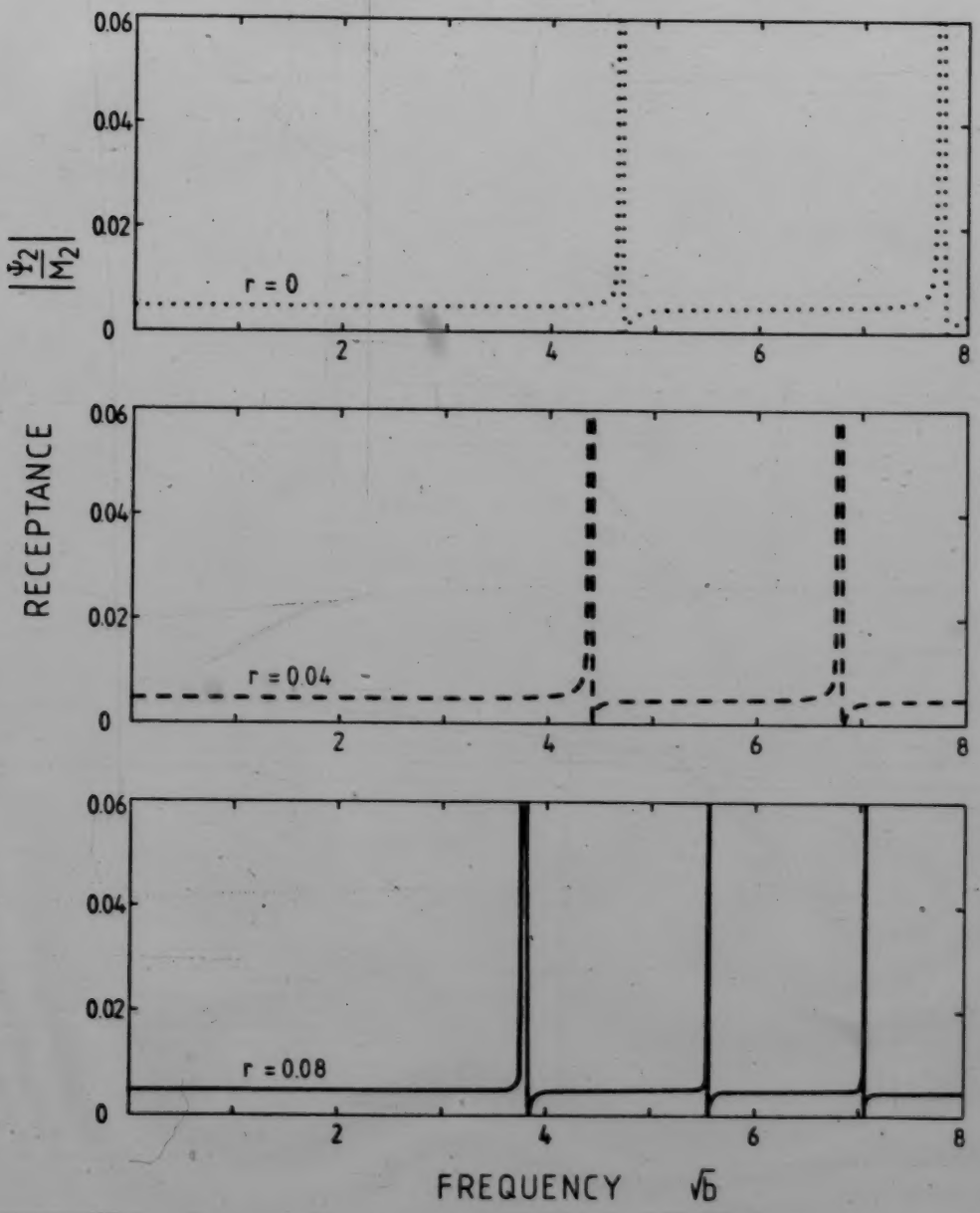

Figure 4.10. continued...

(c) $k_3 = 100.$

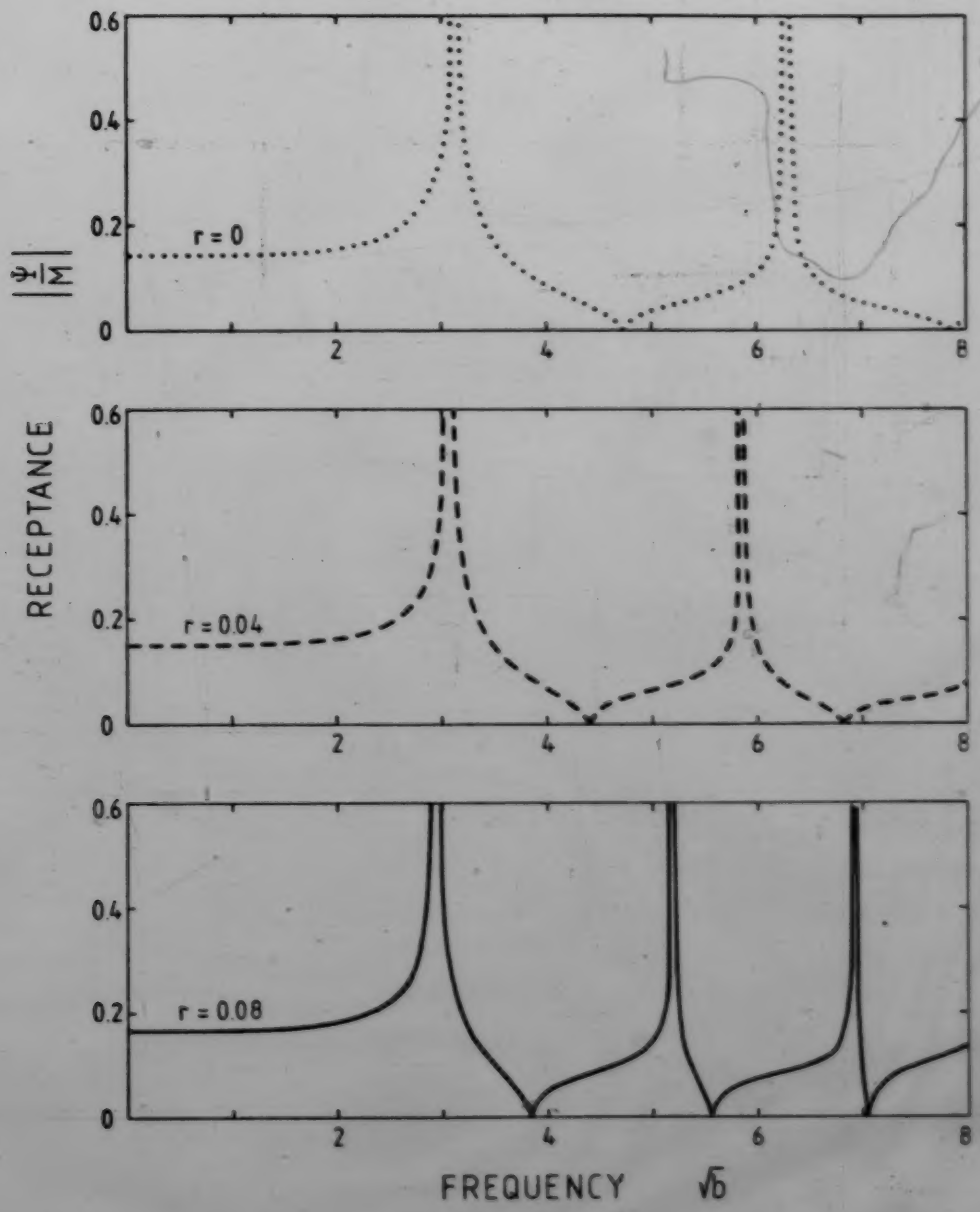

Figure 4.11. Resonance curves of infinite beams on knife-edge supports.

(a) $k_2 = 0$.

2 2
OF / DE

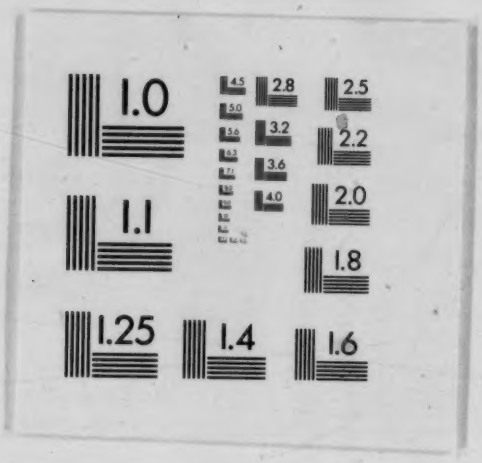

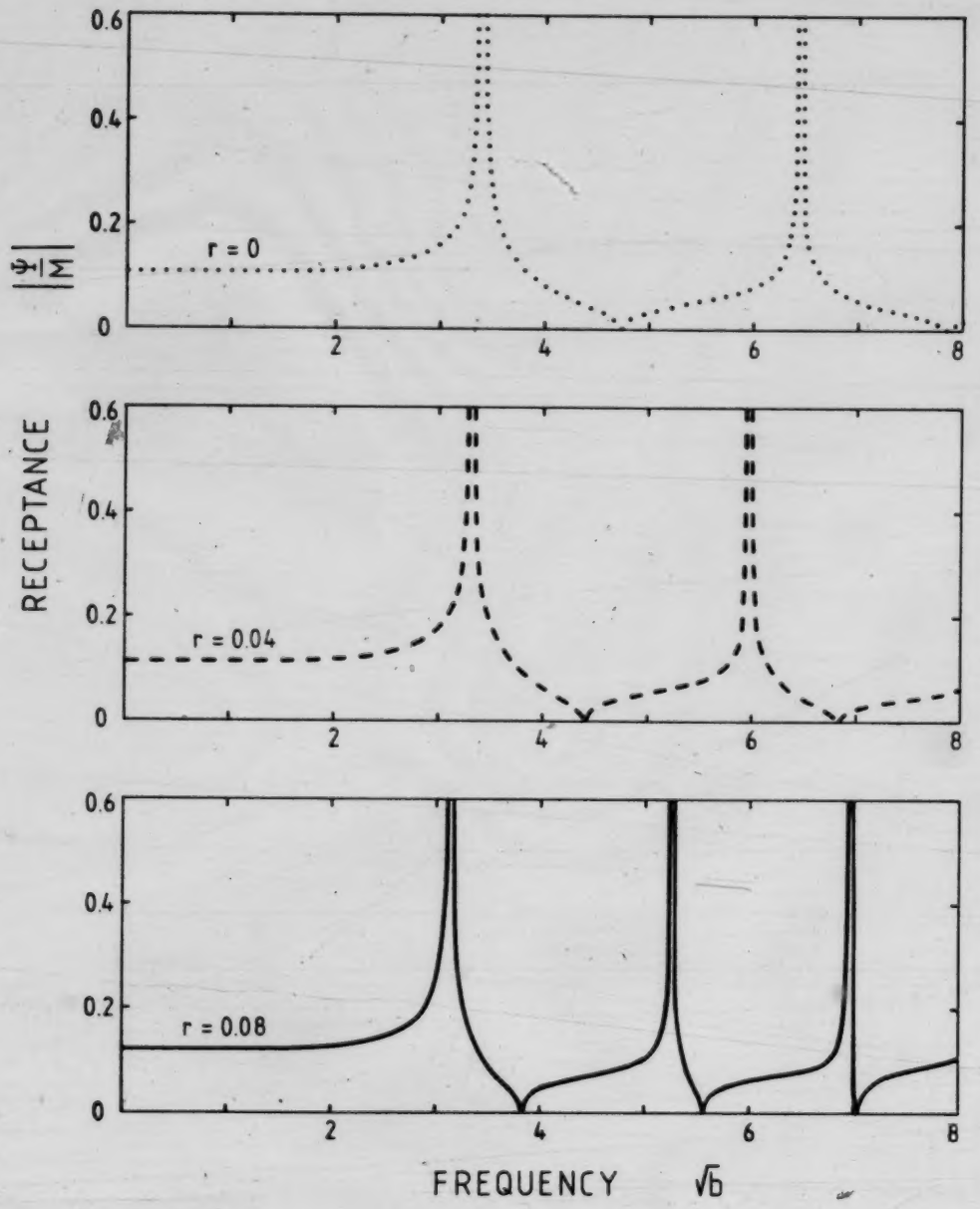

Figure 4.11. continued...

(b) $k_2 = 1$.

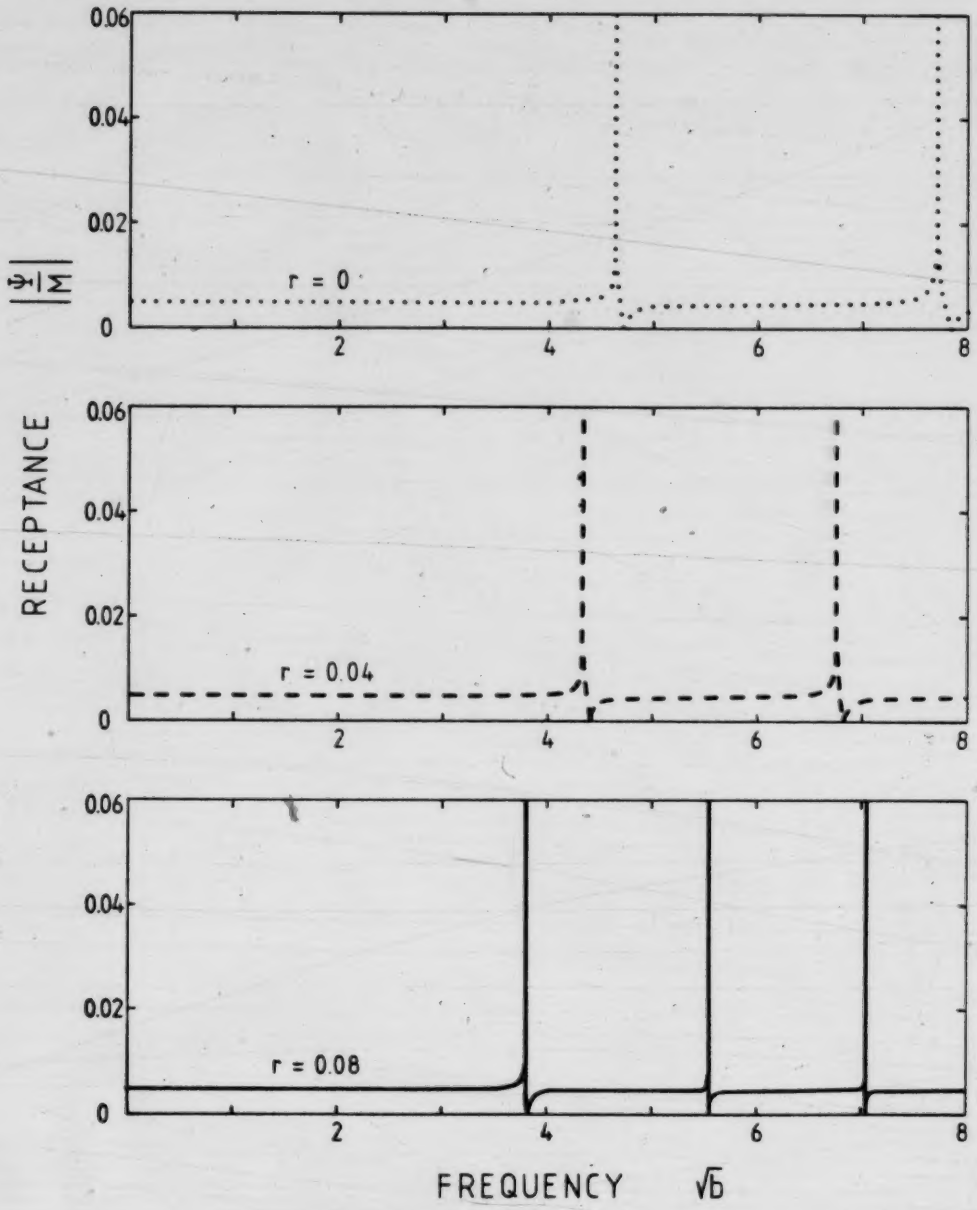

Figure 4.11. continued...

(c) $k_2 = 100.$

Timoshenko beams on elastic springs

Harmonic responses are obtained for the case of vertical force input and deflection output. The results are then shown by the resonance curves - Figures 4.13 and 4.14. A four-span beam with both ends hinged and an infinite beam are taken assuming that the excitation is at the center node of the beams as shown in Figure 4.12.

(a) Four-span hinged-hinged beam.

(b) Infinite-infinite beam.

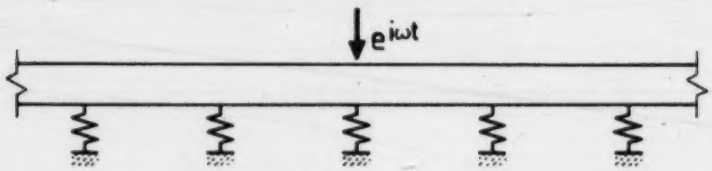

Figure 4.12. Forced vibration of the uniform beams on spring supports.

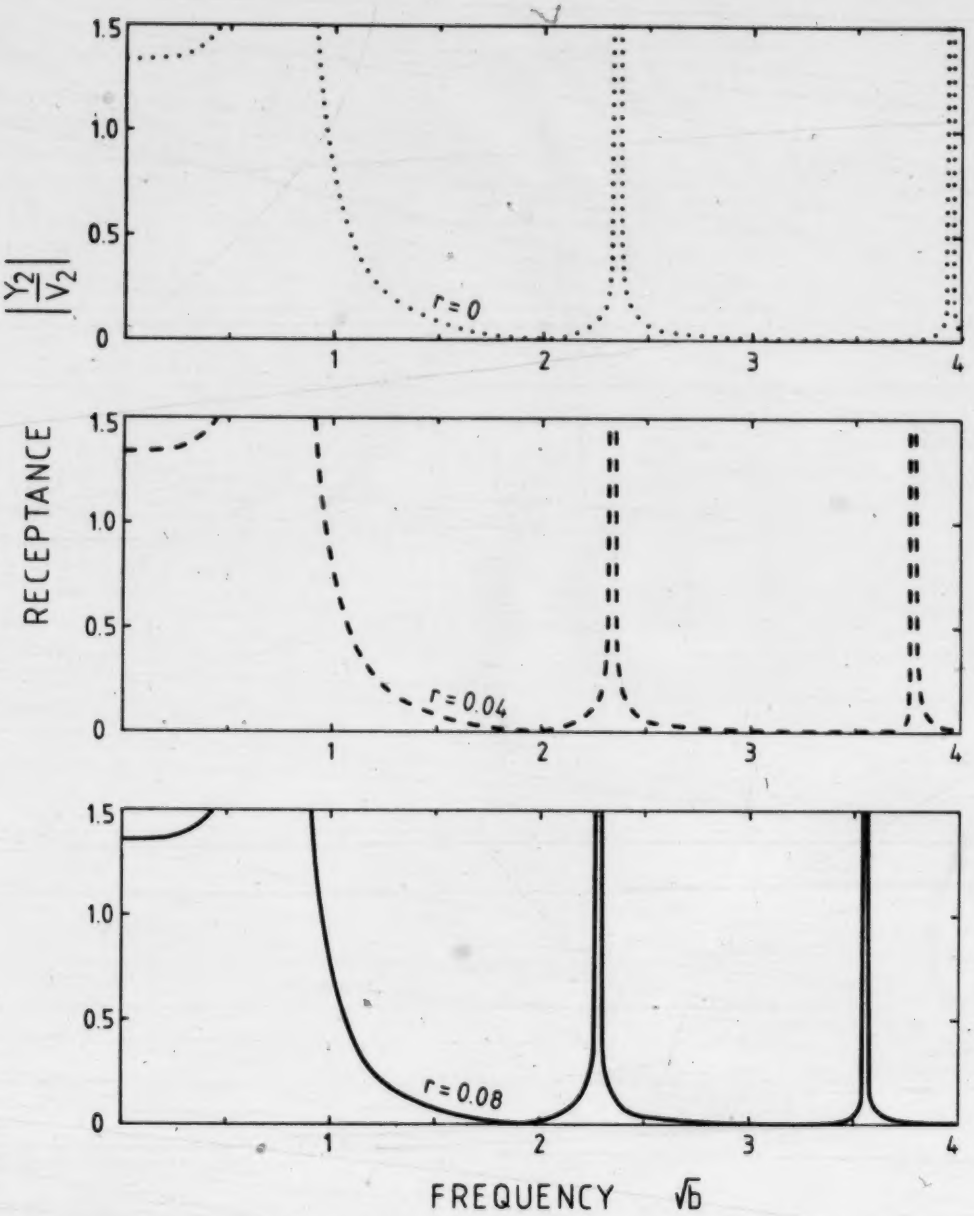

Figure 4.13. Resonance curves for a four span hinged-hinged beams on spring supports.
(a) $k_1 = 0$.

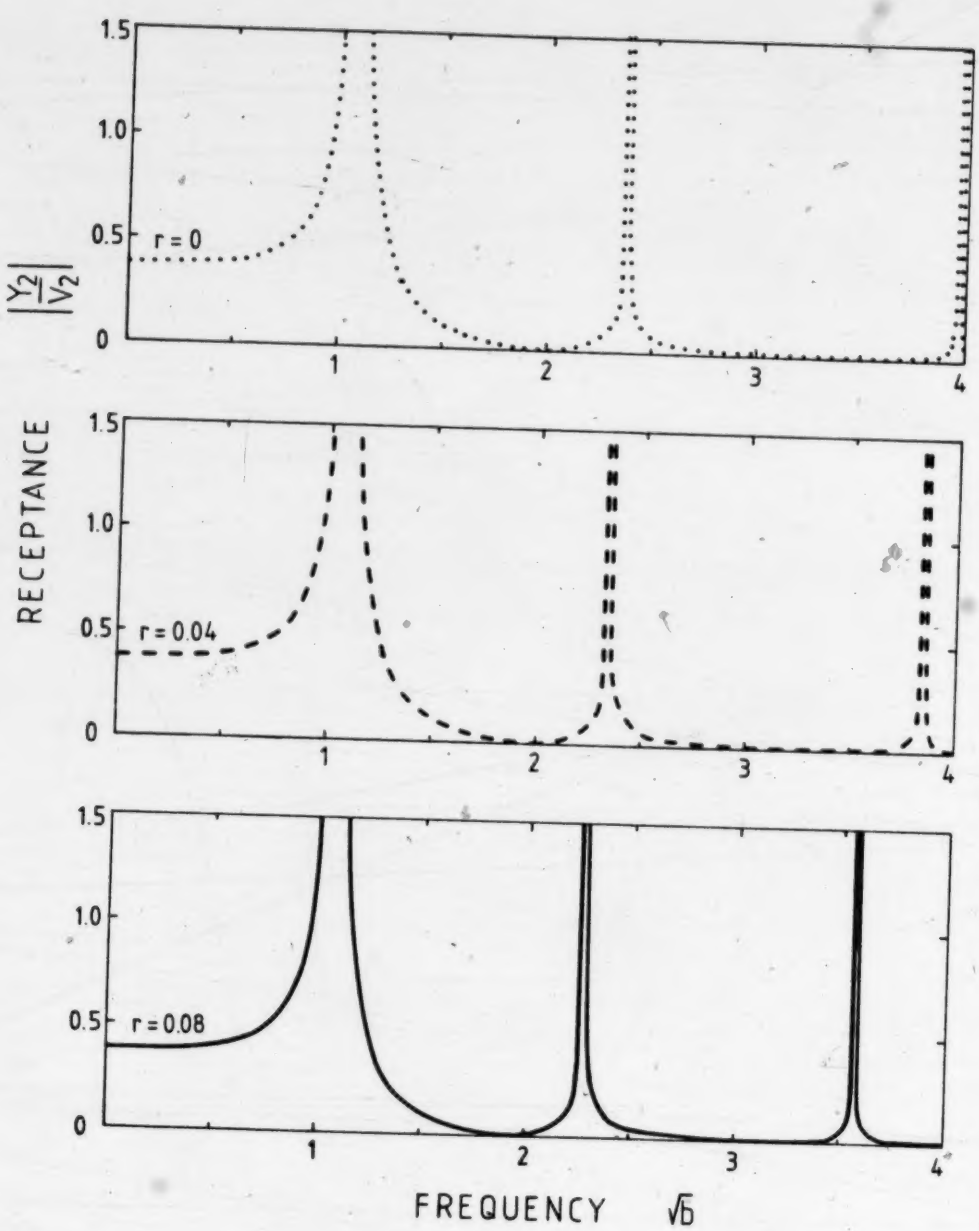

Figure 4.13. continued...

(b) $k_1 = 0.5$.

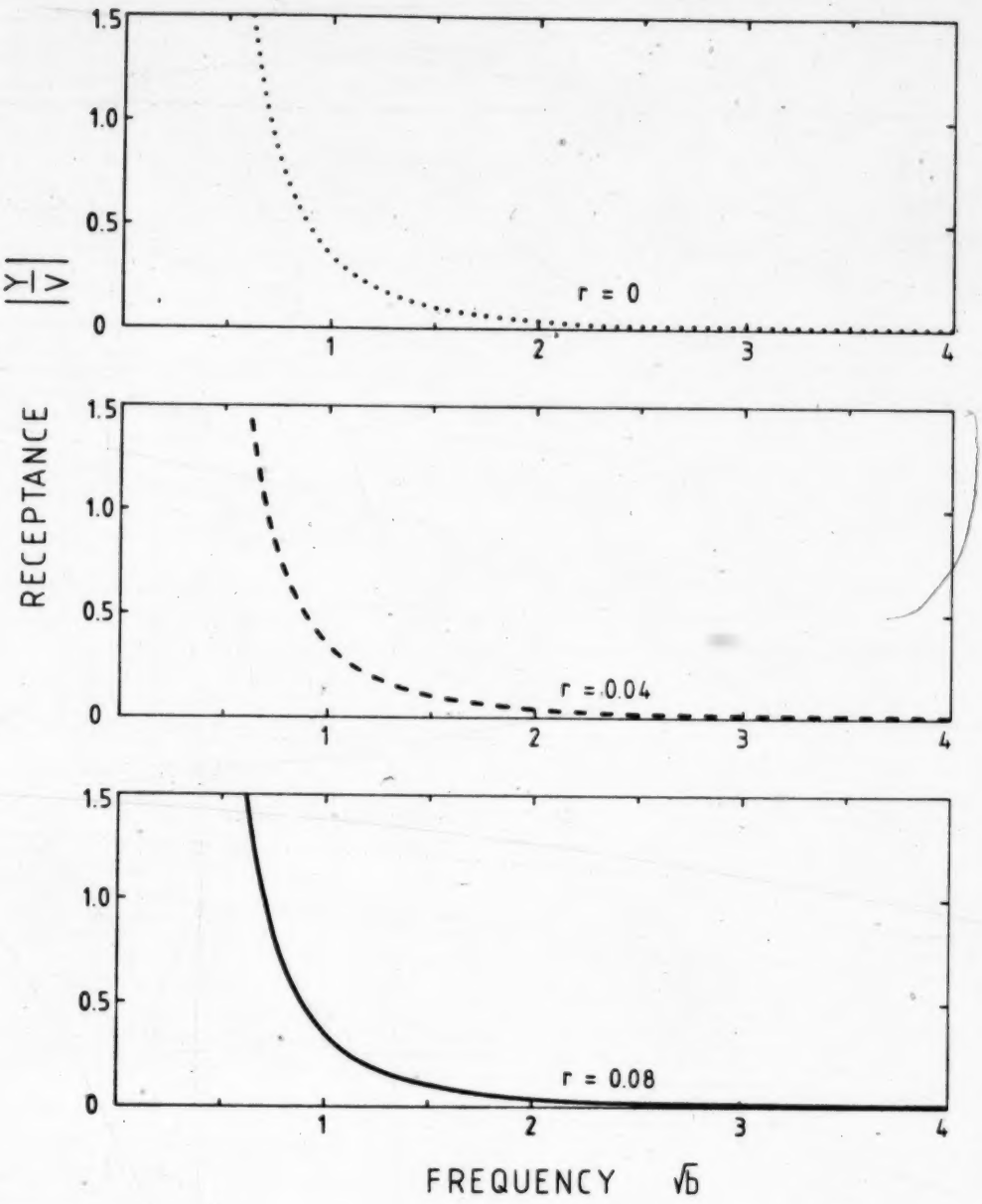

Figure 4.14. Resonance curves for an infinite beam on spring supports.

(a) $k_1 = 0$.

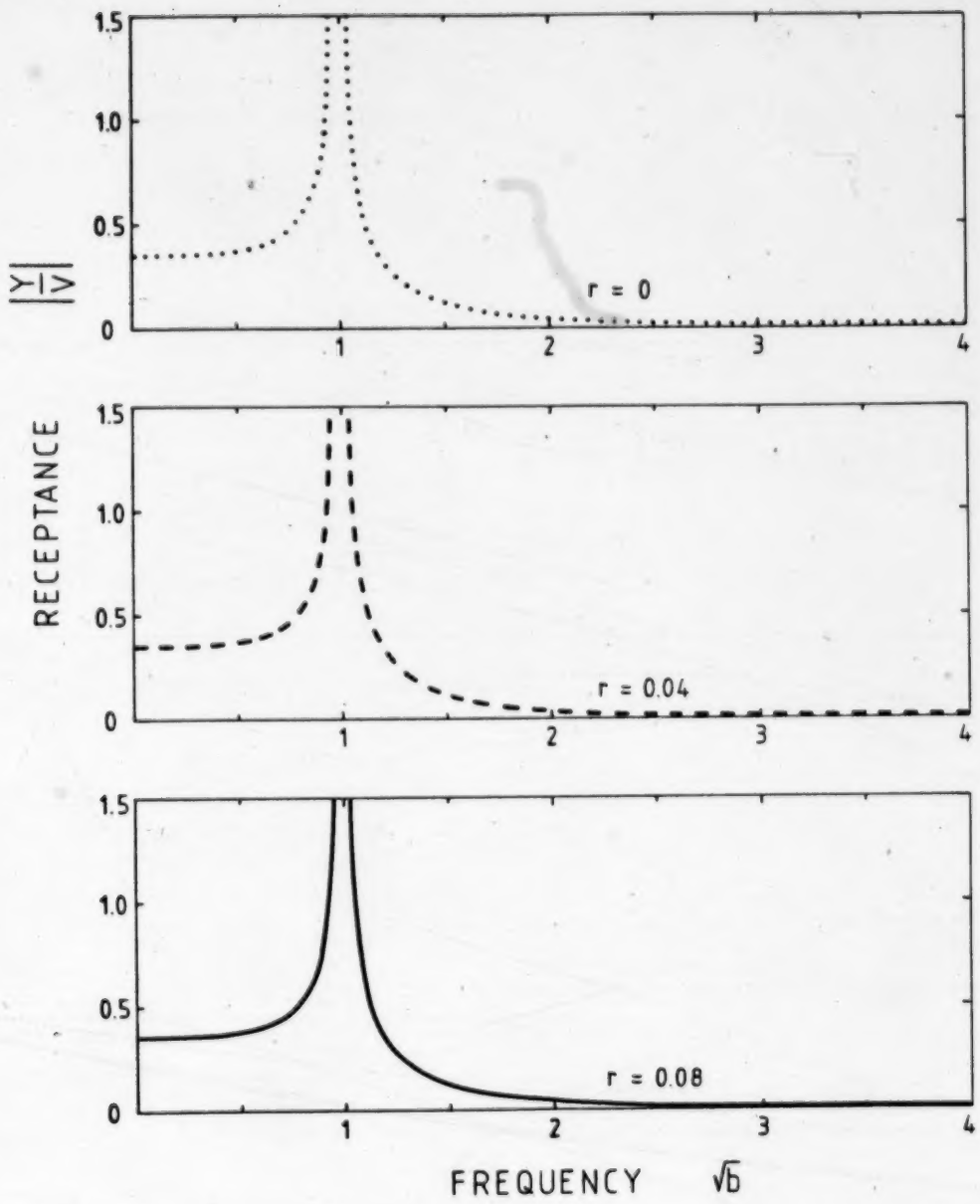

Figure 4.14. continued...

(b) $k_1 = 0.5$.

F. Numerical Results by Finite Element Method

In order to compare the results analytically obtained with those from the Finite Element formulation, a span of the Timoshenko beam on intermediate supports is subdivided into a number of elements. The beam may thus be considered an example of the compound periodic structure - see Figure 4.15.

(a) Element division.

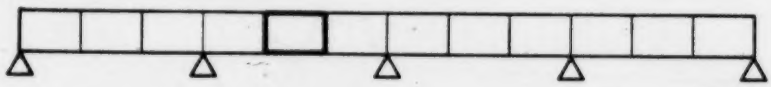

(b) Craggs' element showing the nodal displacements.

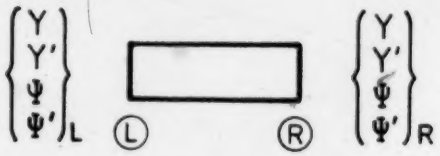

Figure 4.15. Timoshenko beam element for the Finite Element Method.

Craggs' Timoshenko beam element [4] uses four nodal degrees of freedom, namely, the total deflection, Y, bending slope, Ψ and their first derivatives at each end of the element. In between the nodes the total deflection and the bending slope are interpolated by a cubic function from the nodal values. Through the general Finite Element procedure the impedance matrix is then obtained for the beam element

in the nondimensional form as

$$[Z] = [K] - b^2[M] \tag{4.33}$$

where the stiffness matrix, $[K] = \frac{1}{420s^2} \cdot$

$$\begin{bmatrix}
504 & 42 & 210 & 42 & -504 & 42 & 210 & -42 \\
 & 56 & -42 & 0 & -42 & -14 & 42 & -7 \\
 & & 504s^2+156 & 42s^2+22 & -210 & 42 & -504s^2+54 & 42s^2-13 \\
 & & & 56s^2+4 & -42 & 7 & -42s^2+13 & -14s^2-3 \\
 & & & & 504 & -42 & -210 & 42 \\
 & & & & & 56 & -42 & 0 \\
 & & \text{Symmetric.} & & & & 504s^2+156 & -42s^2-22 \\
 & & & & & & & 56s^2+4
\end{bmatrix}$$

and the mass matrix,

$$[M] = \frac{1}{420} \cdot \begin{bmatrix}
156 & 22 & 0 & 0 & 54 & -13 & 0 & 0 \\
 & 4 & 0 & 0 & 13 & -3 & 0 & 0 \\
 & & 156r^2 & 22r^2 & 0 & 0 & 54r^2 & -13r^2 \\
 & & & 4r^2 & 0 & 0 & 13r^2 & -3r^2 \\
 & & & & 156 & -22 & 0 & 0 \\
 & & & & & 4 & 0 & 0 \\
 & & \text{Symmetric.} & & & & 156r^2 & -22r^2 \\
 & & & & & & & 4r^2
\end{bmatrix}$$

Here the nondimensional parameters are as defined in

equations (4.10)-(4.12).

Unlike the analytically derived impedance matrix in equation (4.24), this expression for the impedance matrix of size 8x8 can not be used to represent the Bernoulli-Euler beam element by setting r=s=0. Impedance matrix for the Bernoulli-Euler beam is of size 4x4 and may be found in most texts of Finite Element Method.

At a given frequency, b, this impedance matrix can be evaluated numerically and the transfer matrix can be formed using equation (2.8). This element transfer matrix is then multiplied to form the transfer matrix relating the state vectors at the supports. If the beam is supported on the knife-edges as in the case of Figure 4.15, the transfer matrix for a span can be reduced in size by the procedure explained in the Appendix C. From the reduced transfer matrix thus obtained the eigenvalues are calculated and the logarithmns of these eigenvalues yield the propagation constants. In Figure 4.16 the propagation constant for the flexural motion is plotted against frequency for the two slenderness ratios, r=0.04 and 0.08. For each slenderness ratio a span of the beam is divided into one, two and three elements. From these propagation constant curves the natural frequencies are obtained by the graphical method as explained in Section III.D. Table 4.3 gives the results for the hinged-hinged beams in terms of relative errors compared with the exact solutions.

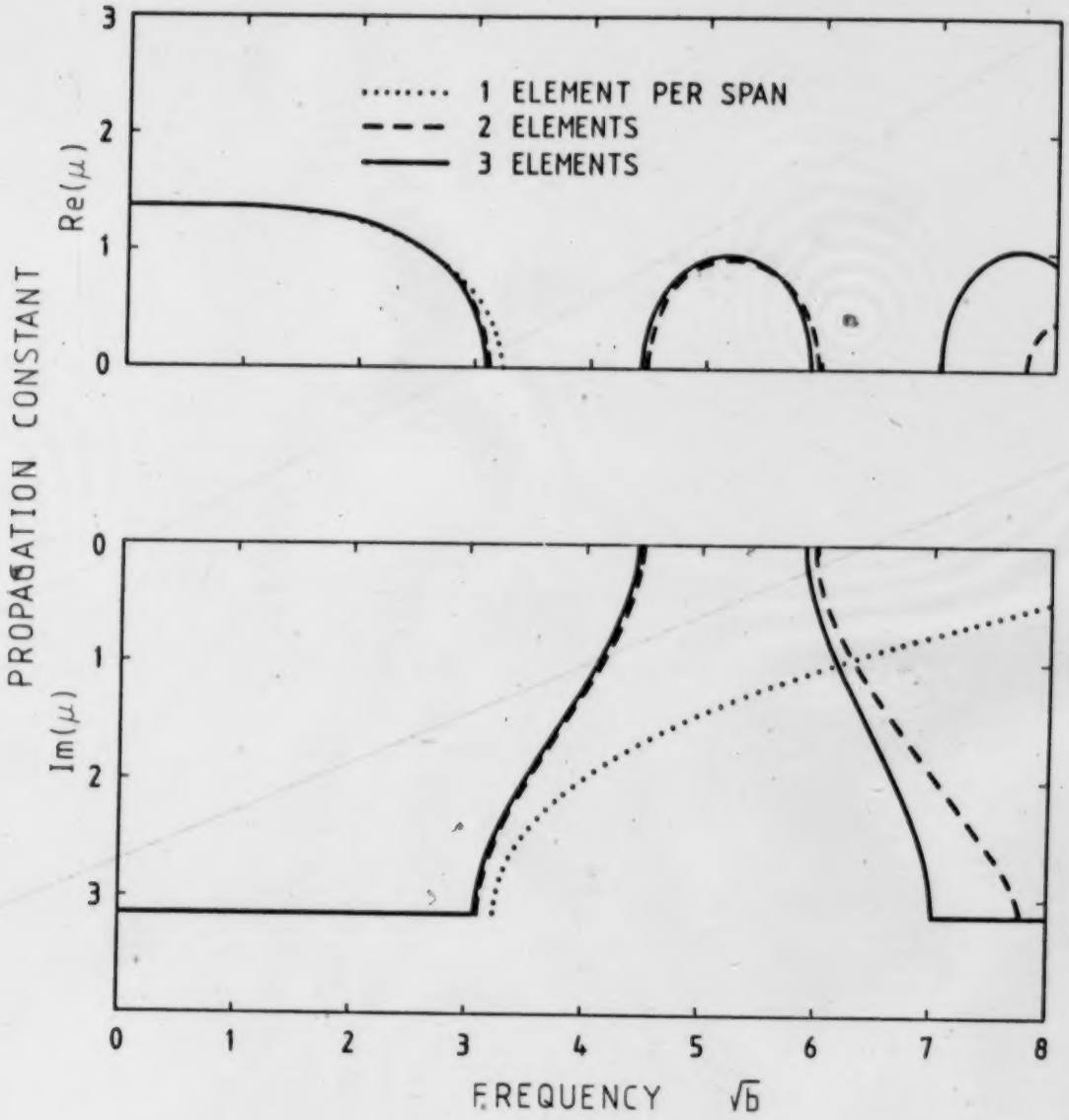

Figure 4.16. Propagation constant by the Finite Element Method. (a) r=0.04.

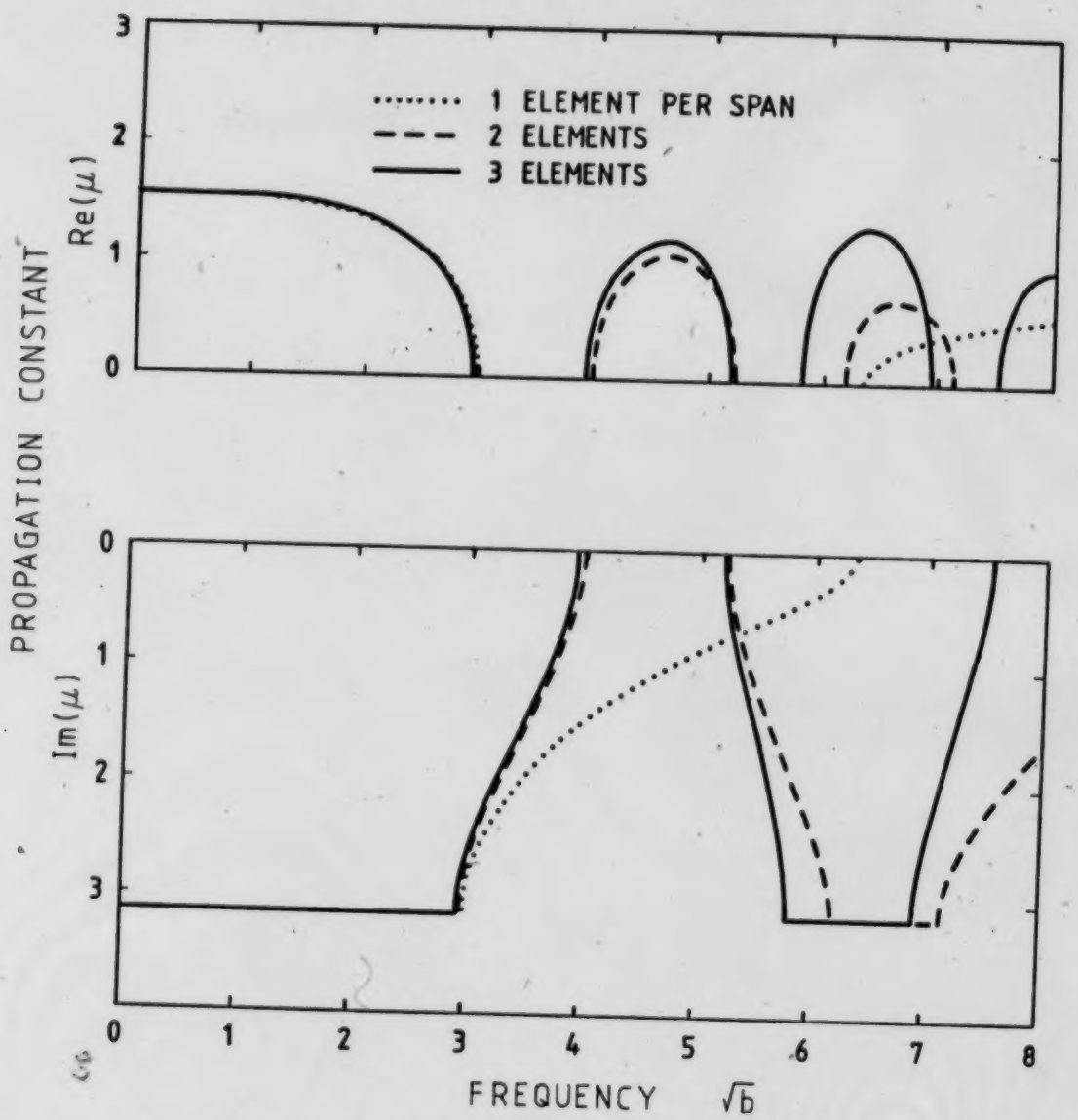

Figure 4.16. continued...

(b) r=0.08.

Table 4.3. Errors of Finite Element results for the four span Timoshenko beam on knife-edge supports.

(a) r = 0.04. (%)

GROUP	MODE	$\sqrt{b}$	NUMBER OF ELEMENTS PER SPAN		
			1	2	3
1	1	3.083	4.7	0.0	0.0
	2	3.301	8.7	0.3	0.1
	3	3.759	25.3	0.7	0.3
	4	4.199	64.9	1.5	0.7
2	5	5.881	-	1.5	0.1
	6	6.046	-	2.6	0.5
	7	6.378	-	5.2	1.2
	8	6.689	-	9.4	2.1

(b) r = 0.08. (%)

GROUP	MODE	$\sqrt{b}$	NUMBER OF ELEMENTS PER SPAN		
			1	2	3
1	1	2.940	1.5	0.0	0.0
	2	3.090	4.0	0.5	0.3
	3	3.412	13.6	1.6	1.0
	4	3.709	38.5	2.9	1.7
2	5	5.192	-	0.6	0.1
	6	5.260	-	1.9	0.7
	7	5.400	-	4.9	2.0
	8	5.520	-	8.6	3.5

G. Discussion

It can be easily shown that the same impedance matrix as in equation (4.7) can be obtained by the classical Finite Element Method using the four normal modes as the interpolation functions, instead of the polynomials. However, this procedure requires more calculation than that is needed by the unknown coefficient method employed in this chapter. If one requires an approximate solution, one can use the polynomials (most commonly cubics) to obtain the impedance matrix in the familiar form as in equation (2.2). The precise method of formulating the impedance matrix is not important in the present study because the present study starts from the impedance matrix. One should be cautious of the sign convention used in the present study because it is consistent with that of Finite Element Method not that commonly used in many texts - see equation (4.18) for example.

Lin[10] used considerable effort to find the expression for $[T^N]$ for the Bernoulli-Euler beam on spring supports. While this approach can also be used for the Timoshenko beam case the Cayley-Hamilton theorem and the similarity transform methods, shown are more efficient. Besides, the present method is aimed at the generally shaped periodic structures not just uniform beams.

As mentioned previously, the four components of the transfer matrix for the mono-coupled systems are in fact the frequency equations for a single span system with different

boundary conditions. Therefore three frequency equations can be obtained for the Timoshenko beams with three different boundary conditions from the transfer matrix in equation (4.31); t_{11} (or t_{22}) for clamped-hinged, t_{12} for clamped-clamped and t_{21} for hinged-hinged case. These frequency equations are the same as those found in [7] except in the case of hinged-hinged boundary, where the two equations yield the same set of solutions in the low frequency range. However, in the high frequency range where the argument of the hyperbolic normal functions, p becomes imaginary number so that these functions in fact become trigonometric, Huang's equation fails to give all the frequency roots.

All the results are obtained for the three slenderness ratios; r=0, 0.04 and 0.08. The nondimensional parameter, s is set to twice these values assuming that the shape factor, k'=2/3 (or 0.65) and E/G=8/3 (or 2.6), which was used in the references.

Figures 4.3-4.5 show the propagation constants for the Timoshenko beam on the knife-edge supports and with the rotational springs, k_2=0, 1 and 100. With r=0 and k_2=0 the propagation constant curve becomes identical to Figure 3.5 and also that in [20] for the Bernoulli-Euler beam. The propagation constant has a repeating regular pattern of interval 2π, with the propagation zones lying in the frequency ranges $m\pi \le \sqrt{b} \le (m+0.5)\pi$, approximately. Therefore, once the natural frequencies of the first group are

obtained, the higher group natural frequencies are simply obtained by adding multiples of π to these frequencies. This regular pattern becomes distorted as the slenderness ratio increases by shifting the curve towards the lower frequency side, that is, the natural frequency becomes lower with increasing slenderness ratio. Above a certain frequency the alternating pattern of attenuation and propagation zones completely breaks and there can be an additional natural frequency in a group.

The increase in the rotational spring constant, k_2 makes the propagation zone narrower by moving the lower bounding frequency towards the upper bounding frequency giving higher natural frequencies. Since the upper bounding frequencies are the natural frequencies of the single span clamped-clamped beam, these are independent of the rotational spring, k_2. The lower bounding frequencies, on the other hand, which are the natural frequencies of the single span hinge-hinged beam for which the ends can rotate, increase for the higher k_2. As k_2 increases further these natural frequencies approach the upper bounding frequencies of the propagation zones which are the natural frequencies of the single span beam with both ends clamped. The propagation of the flexural waves is then possible only at these frequencies and every span of the beam becomes virtually isolated.

In the case of beams on spring supports, little is to be gained by considering the propagation constant and the

natural frequencies are found by iteratively solving the frequency equations. The results are shown in Table 4.2. With both k_1 and k_2 being zero the beam becomes a single span beam with no intermediate supports, which is identical to the beam considered in [7]. The propagation constants in this case are $\mu=\pm p, \pm qi$ and the natural frequencies are $j\pi/N$ $(j=1,2,...)$ for the Bernoulli-Euler beam with both ends hinged; and approximately $(j+0.5)\pi/N$ $(j=1,2,...)$ for the clamped-clamped case. The reason that the number of spans, N appear in these frequencies is that the frequency parameter b is based on the beam element length.

By increasing the translational spring constant, k_1, the natural frequencies increase approaching the natural frequencies of the beams on knife-edge supports. The effect of the rotational spring would be higher natural frequencies, however, it is not considered in this case.

The total deflections shown in the mode shapes in Figure 4.6 and 4.8 are identical to those for the Bernoulli-Euler beams except that the total deflection of the Timoshenko beam is composed of deflections due to bending and shear. When the mode shapes are simple sinusoidal curves as the first mode in Figure 4.6 and all the modes in Figure 4.8, there exists a constant which governs the proportion of the deflections due to bending and shear throughout the beam. The proportion of the shear deformation increases as the frequency increases and at the sufficiently high frequency normal modes of pure shear can

appear. The translational or the rotational springs at the supports do not affect the mode shapes.

The effect of the rotary inertia and shear deformation on the natural frequencies is shown in the form of a correction factor given in Figure 4.17. The corrections for the single span hinged-hinged beam are similar to those for clamped-free beam as shown in [7]. In the case of the four span beam, the corrections for the first four modes fall in between those of the first and second mode of the single span beam.

There are two resonances and two zero responses in each frequency band in Figures 4.10 and 4.11. A four-span beam has four natural frequencies, of which two correspond to symmetric modes, the other two to anti-symmetric modes. Since the external moment is applied at the center node, it only excites the anti-symmetric modes. Hence the resonance occurs at these two natural frequencies corresponding to anti-symmetric modes and the bending slope vanishes at the center at the natural frequencies corresponding to symmetric modes. It is obvious then that the number of these resonances and zero receptances in each group increases with the number of spans, making the analysis very difficult as a slight change in the frequency results in the change of response from zero to infinite or vice versa. Therefore it is more convenient to assume the number of spans being infinite in this circumstance, which not only saves the computational efforts but yields reasonable results as shown

(a) Single span beam.

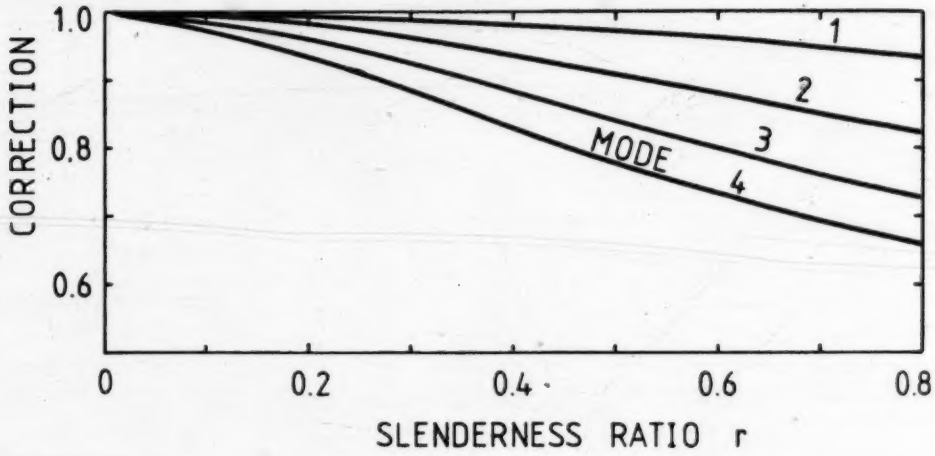

(b) Four span beam.

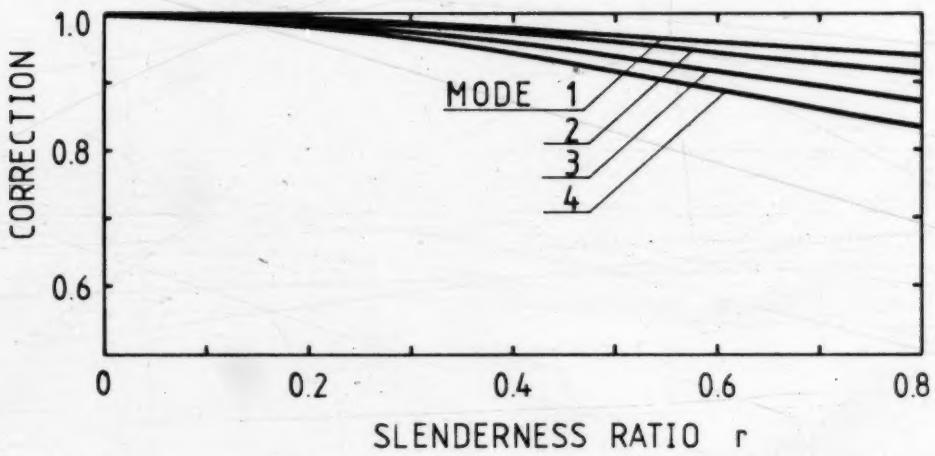

Figure 4.17. Effect of rotary inertia and shear deformation on the natural frequencies of hinged beams.

in Figure 4.11. In the case of infinite beams there is a single resonance and a zero receptance in each frequency band; the resonating frequency is the natural frequency of a single span beam with both ends hinged, and zero receptance at the natural frequency of a clamped-clamped beam element smoothing the response in between these two bounding frequencies. A similar trend can be observed in Figures 4.13 and 4.14, which show the vertical deflection due to vertical excitation introduced at the center nodes of a four-span beam and an infinite beam on elastic springs. The response does not have to be found only at the point of excitation. The state vectors at any nodes can be obtained by equation (3.12), once the equation (3.11) is solved, since the upper half of the entries in the state vectors are the displacement responses. The harmonic response problems considered are for the cases of force-input displacement-output problems. However, since the input vector {w} in equation (3.11) contains both the displacement and force terms, the opposite case can also be treated in identical ways. In fact even the mixed input problems can be considered, however, it is rare to find such applications in practice.

It should be noted that the response at zero frequency is in fact the response due to the static force. Hence the present method of analysis does not exclude the static analysis of periodic structures.

Whether the impedance matrix is obtained analytically or by the Finite Element Method, the transfer matrix analysis is identically applied in the present study. This was demonstrated by using the impedance matrix in reference [4]. The accuracy of the Finite Element solution depends largely upon how closely the interpolation function can approximate the true shape of the normal modes. If the cubic function is used as with the Craggs' element, the function may not satisfactorily approximate the deformation corresponding to the second or higher group natural modes. Therefore only the first group of natural frequencies are obtained with a single element per span. As the number of elements per span increases the propagation constant curve from the Finite Element more closely resembles that of the analytically obtained.

Generally, the accuracy of the Finite Element solution deteriorates as the frequency increases. For the multi-span beam, however, the accuracy the lower mode solution in the next group is better than that of the last mode in the previous group. This can be also noted in the propagation constant curve. In each propagation zone the discrepancy increases with the frequency but the discrepancy at the lower bounding frequency of the next propagation zone is smaller than that at the upper bounding frequency.

The same four span Timoshenko beam was also treated by the ordinary Finite Element Method. The natural frequencies were obtained by finding the eigenvalues, b^2 from the global

impedance matrix assembled from the element impedance matrices. The solutions by this ordinary Finite Element Method are the same as those obtained through the formulation of the transfer matrix within the round-off error. The advantage of the present method of analysis is then the computational efficiency. The computing time (CPU) required for these two methods is shown in Figure 4.18. which represents only the specific case of the example in the present study. However, the general trend can be observed indicating that the increasing computational effort is necessary to obtain better solutions by the ordinary Finite Element Method. On the other hand, the computational effort is virtually constant regardless of number of elements per span when the transfer matrix method is used.

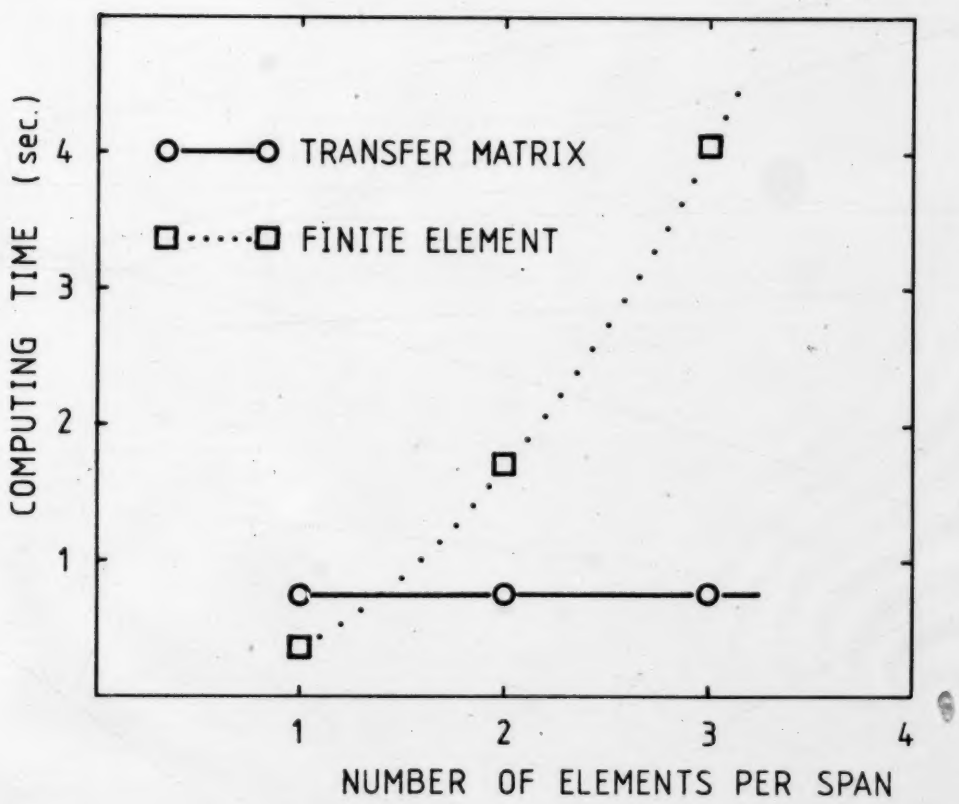

Figure 4.18. Comparison of the computing time used.

V. CONCLUDING REMARKS

There have been two different approaches used for the vibration analysis of periodic structures; the matrix method and the wave approach. The present method is a blending of these two approaches putting more emphasis on the transfer matrix and merging the properties of propagation constants and the eigenvalues of the transfer matrix. Since periodic structures can be of complex shapes so that the analysis can be done by numerical means only, the transfer matrix in the present study is derived from the impedance matrix which commonly formulated by the Finite Element Method. These ideas are not really new and had been used by previous authors. However, the present study is somewhat more complete and easier to implement since the method suggested is quite general, efficient but very simple. Some of the advantages of the present study which have been discussed in the previous chapters are:

1. The periodic structure can be of any complex form. Many other methods are only applicable to specific type of periodic structure, but the present study can handle a periodic structure composed of different substructures, or a structure which is not even periodic at all. The periodic unit can be either symmetric about its center or unsymmetric.
2. The periodic structure may have any type of extreme boundaries. Even the infinite structures can be handled by the present method, which can not be analyzed by

other matrix methods. The wave approach on the other hand can not satisfactorily handle the ordinary boundary conditions.

3. Free or forced vibration analyses are performed with practically the same procedure. Other methods usually can handle either free or forced analysis.

4. As many natural frequencies as needed or those in the specific frequency ranges can be obtained by the present method. The Finite Element Method, on the other hand, yields only the same number of natural frequencies as the size of matrix starting always from the lowest natural frequency.

5. The results can be obtained either analytically or numerically, depending on what type of impedance matrix used. Other studies are commonly directed to just one of these. The method yields accurate results without any complicated measures of avoiding errors due to the digital computations. This is accomplished by reducing the computational effort to a minimal amount.

Any periodic structure can be taken as the numerical example for the present study. However, it is believed that the results for the Timoshenko beams on multiple supports are readily applicable to practical engineering problems. These results are more useful for the short and stubby beams and for the high frequency analysis, where the Bernoulli-Euler beam theory fails to give acceptable results.

In the cases where the high frequency vibration is concerned or the periodic structure contains many bays, the damping effect may be noticeable and the analysis should include the damping terms. Further study may be directed to understanding of the wave phenomena in terms of the propagation constant and the transfer matrices. It may be also possible to extend the application of the present study to engineering problems other than the static and dynamic analysis of the structures, such as heat transfer, fluid flow or some other problems which can be expressed in the form of difference equations.

BIBLIOGRAPHY

1. Ayre, R. S. and Jacobsen, L. S., *Natural frequencies of continuous beams of uniform span length, J. Appl. Mech.* 17, 1950, 391-395

2. Bishop, R. E. D. and Johnson, D. C., The Mechanics of Vibration, Cambridge Univ. Press, 1966

3. Brillouin, L., Wave Propagation in Periodic Structures, Dover publication, New York, 1953

4. Craggs, A., An Accurate Timoshenko Beam Finite Element, Dept. Mech. Eng., Univ. of Alberta, 1980

5. Denke, P. M., Eide, G. R. and Pickard, J. *Matrix difference equation analysis of vibrating periodic structures, AIAA J.* 13, 1975, 160-166

6. Heckl, M., *Wave propagation in beam-plate systems, J. Accoust. Soc. Am.* 33, 1961, 640

7. Huang, T. C., *The effect of rotatory inertia and of shear deformation on the frequency and normal mode equations of uniform beams with simple end conditions, J. App. Mech., Trans ASME*, 28, 1961, 579-584

8. Kapur, K. K., *Vibrations of a Timoshenko beam using Finite-Element Approach, J. Accoust. Soc. Am.* 40(5), 1966, 1058-1063

9. Lin, Y. K., *Free vibration of a continuous beam on elastic supports, Int. J. Mech. Sci.* Vol. 4, 1962, 409-423

10. Lin, Y. K. and McDaniel, T. J., *Dynamic of beam type periodic structures, J. Eng. for Ind. Trans ASME*, Nov. 1969, 1133-1141

11. Mead, D. J., *Free wave propagation in periodically supported, infinite beams, J. Sound. Vib.* 11, 1970, 181-197

12. Mead, D. J., *Vibration response and wave propagation in periodic structures, J. Eng. Ind., Trans. ASME* 93, 1971, 783-792

13. Mead, D. J., *Wave propagation and natural modes in periodic systems:*
I. Mono-coupled systems
II. Multi-coupled systems, with and without damping, J.

Sound Vib. 40(1), 1975, 1-18, 19-39

14. Meirovitch, L. and Engels, R. C., *Response of periodic structures by the Z-transform method, AIAA J.* 15, 1977, 167-174

15. Meirovitch, L. and Engels, R. C., *Response of periodic structures by modal analysis, J. Sound Vib.* 56(4),1978, 481-493

16. Miles, J. W., *Vibrations of beams on many supports, Proc. Am. Soc. Civil Engrs.* Vol. 82, 1956, 1-9

17. Orris, R. M. and Petyt, M., *Random response of periodic structures by a finite element technique, J. Sound Vib.* 43(1),1975, 1-8

18. Pestel, E. C. and Leckie, F. A., Matrix Methods in Elastomechanics, McGraw-Hill, New York, 1963

19. Sen Gupta, G. S., *Natural flexural waves and the normal modes of periodically supported beams and plates, J. Sound Vib.* 13(1), 1970, 89-101

20. Sen Gupta, G. S., *Natural frequencies of periodic skin-stringer structures, using a wave approach, J. Sound Vib.* 16, 1971, 567-580

21. Timoshenko, S., Young, D. H. and Weaver, W. Jr., Vibration Problems in Engineering, 4th Ed., John Wiley & Sons, Inc., 1974, 432-435

VI. APPENDIX

A. Impedance matrices for spring-mass systems

1) System of symmetric elements

It can be shown that the mass and the stiffness matrices can be expressed for the symmetric element shown in Figure 3.3(a) in the form

$$[M] = m\begin{bmatrix} 1 & 0 \\ 0 & 1 \end{bmatrix}, \tag{6.1}$$

$$[K] = k\begin{bmatrix} 1 & -1 \\ -1 & 1 \end{bmatrix}. \tag{6.2}$$

The impedance matrix is then expressed in the nondimensional form as

$$[Z] = \begin{bmatrix} 1-b^2 & -1 \\ -1 & 1-b^2 \end{bmatrix} \tag{6.3}$$

where $b^2=m\omega^2/k$. Using this impedance matrix and the procedure described in equation (2.8), the transfer matrix as in equation (3.24) is obtained.

2) System of unsymmetric elements

For the unsymmetric element the mass and the stiffness

matrices can be obtained as

$$[M] = m\begin{bmatrix} 2 & 0 \\ 0 & 0 \end{bmatrix}, \tag{6.4}$$

$$[K] = k\begin{bmatrix} 1 & -1 \\ -1 & 1 \end{bmatrix}. \tag{6.5}$$

The impedance matrix in this case becomes

$$[Z] = \begin{bmatrix} 1-2b^2 & -1 \\ -1 & 1 \end{bmatrix}. \tag{6.6}$$

From this impedance matrix, the transfer matrix in equation (3.29) is obtained.

B. Derivation of transfer matrix by direct method

The nondimensional shear force and the bending moment shown in Figure 4.1 can be evaluated from equation (4.19) including the terms due to springs, k_1 and k_2 as

$$\begin{aligned} V &= b^2r^2\Psi+\Psi''+k_1Y \\ M &= -\Psi'+k_2\Psi, \end{aligned} \tag{6.7}$$

at $\xi=0$, and

$$\begin{aligned} V &= b^2r^2\Psi+\Psi''-k_1Y \\ M &= -\Psi'-k_2\Psi, \end{aligned} \tag{6.8}$$

at $\xi=1$.

Thus the state vectors at $\xi=0$ and $\xi=1$ can be written in terms of the normal mode functions and the coefficients, $\{C\}$ as

$$\{v\}_0 = \begin{bmatrix} 1 & 0 & 1 & 0 \\ 0 & \alpha & 0 & \beta \\ k_1 & q\alpha\beta & k_1 & -p\alpha\beta \\ -p\alpha & k_2\alpha & q\beta & k_2\beta \end{bmatrix} \begin{Bmatrix} C_1 \\ C_2 \\ C_3 \\ C_4 \end{Bmatrix} \tag{6.9}$$

$$\{v\}_1 = \begin{bmatrix} Ch & Sh & C & S \\ \alpha Sh & \alpha Ch & -\beta S & \beta C \\ q\alpha\beta Sh-k_1Ch & q\alpha\beta Ch-k_1Sh & p\alpha\beta S-k_1C & p\alpha\beta C-k_1S \\ -p\alpha Ch-k_2\alpha Sh & -p\alpha Sh-k_2\alpha Ch & q\beta C-k_2\beta S & q\beta S-k_2\beta C \end{bmatrix} \begin{Bmatrix} C_1 \\ C_2 \\ C_3 \\ C_4 \end{Bmatrix}. \tag{6.10}$$

The matrix in equation (6.10) is postmultiplied by the inverse of the matrix in equation (6.9) to yield the expression for the transfer matrix identical to equation (4.28).

C. Derivation of the reduced transfer matrix

The transfer matrix for the beam on knife-edge supports can be obtained from that for the beam on spring supports in equation (4.28) by eliminating the components corresponding to the deflection, Y and the shear force, V. Since the deflection, Y is not permitted on the knife-edge supports

$$Y = 0 = t_{12}\Psi + t_{13}V + t_{14}M, \tag{6.11}$$

where t_{ij} denotes the i-th row and j-th column entry of the transfer matrix in equation (4.28) with $k_1=0$. The third column of the transfer matrix then can be replaced by the relationship obtained in equation (6.11) leaving the reduced matrix of size two as

$$[T] = \begin{bmatrix} t_{22} & t_{24} \\ t_{42} & t_{44} \end{bmatrix} - t_{13}^{-1} \begin{Bmatrix} t_{23} \\ t_{43} \end{Bmatrix} [t_{12} \quad t_{14}]. \tag{6.12}$$

The transfer matrices in equations (4.31) and (4.32) are obtained by this procedure from the transfer matrices in equations (4.28) and (4.29).